Theories of VHE emission from pulsar magnetospheres

Kouichi HIROTANI

ASIAA,Taiwan

TeVPA 2015

Kashiwa, Japan

October 27, 2015

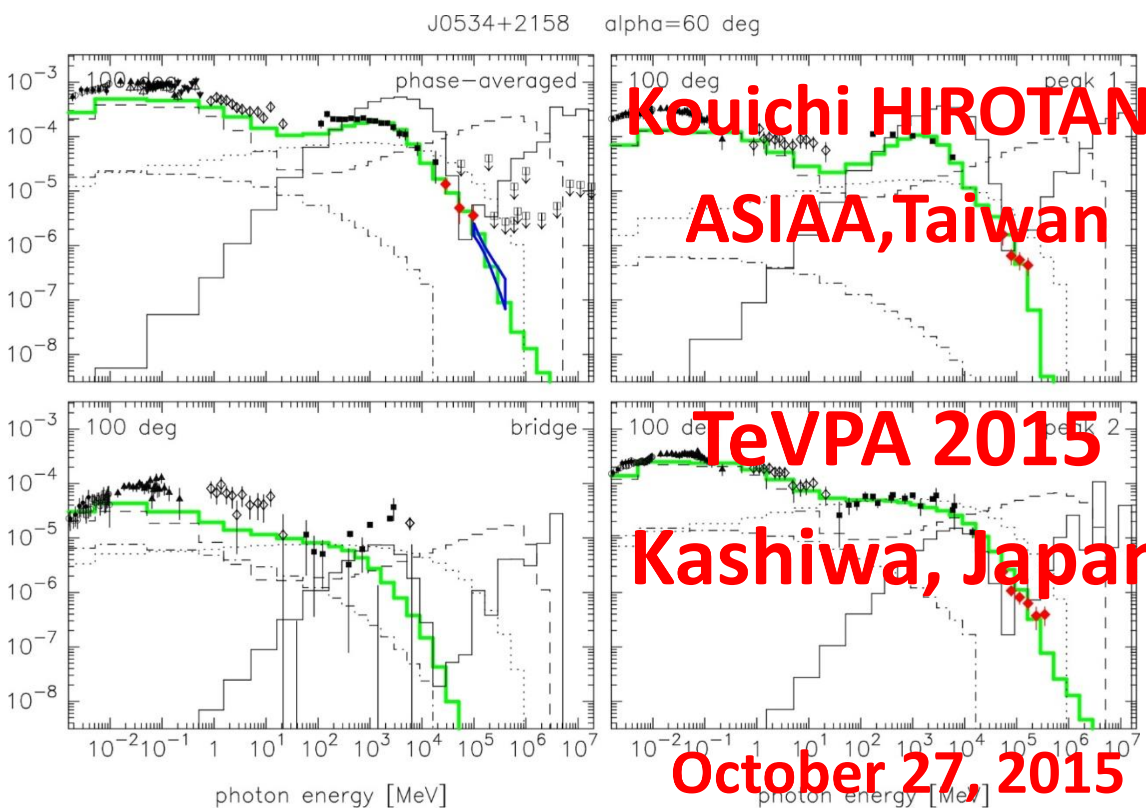

+BH (IC 310)

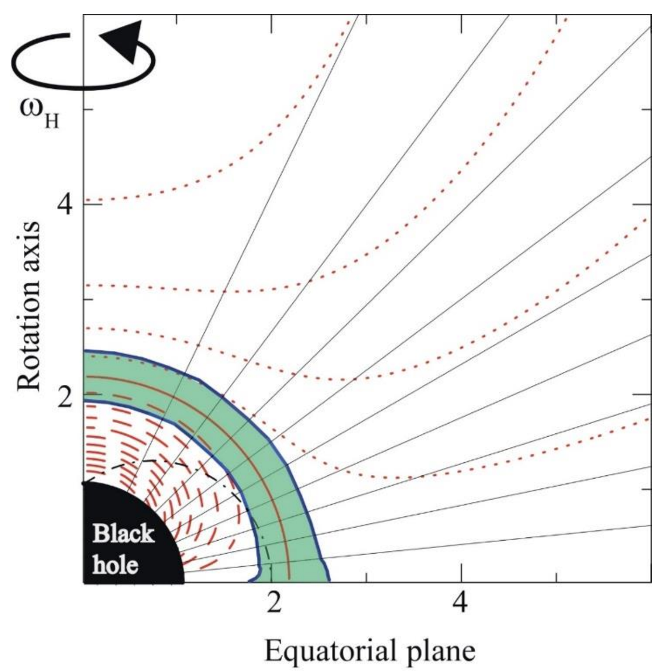

§1 γ-ray Pulsar Observations

After 2008, LAT aboard Fermi has detected more than 117 pulsars above 100 MeV.

Fermi/LAT point sources (>100 MeV)

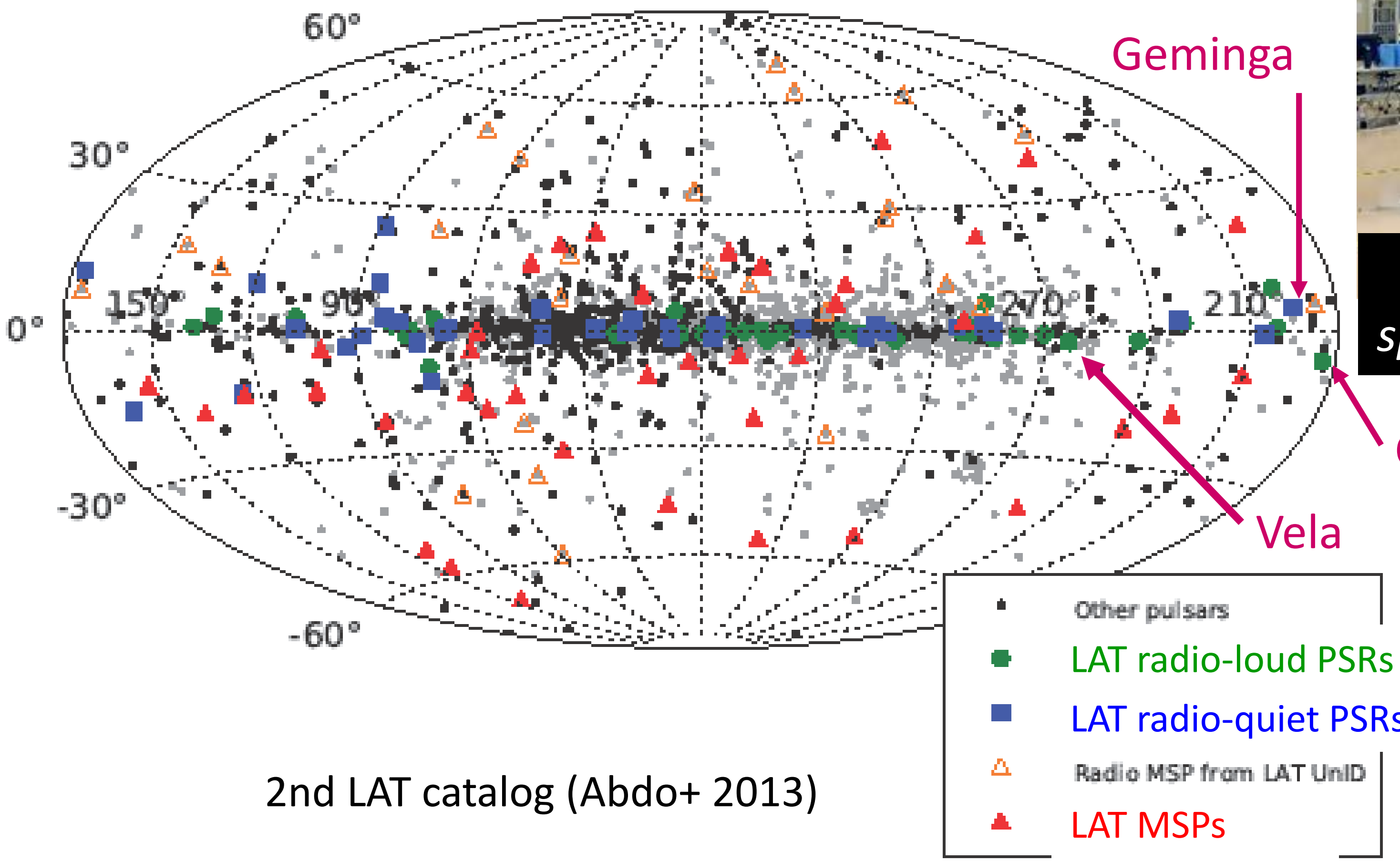

2nd LAT catalog (Abdo+ 2013)

Pulsed broad-band spectra of young pulsars

- High-energy (~GeV) photons are emitted mainly via **curvature** process by ultra-relativistic, primary *e*⁻'s/e⁺'s.

(created in particle accelerator)

- However, > 20 GeV, **Inverse-Compton scatterings (ICS) by the cascaded *e*±'s** contribute.

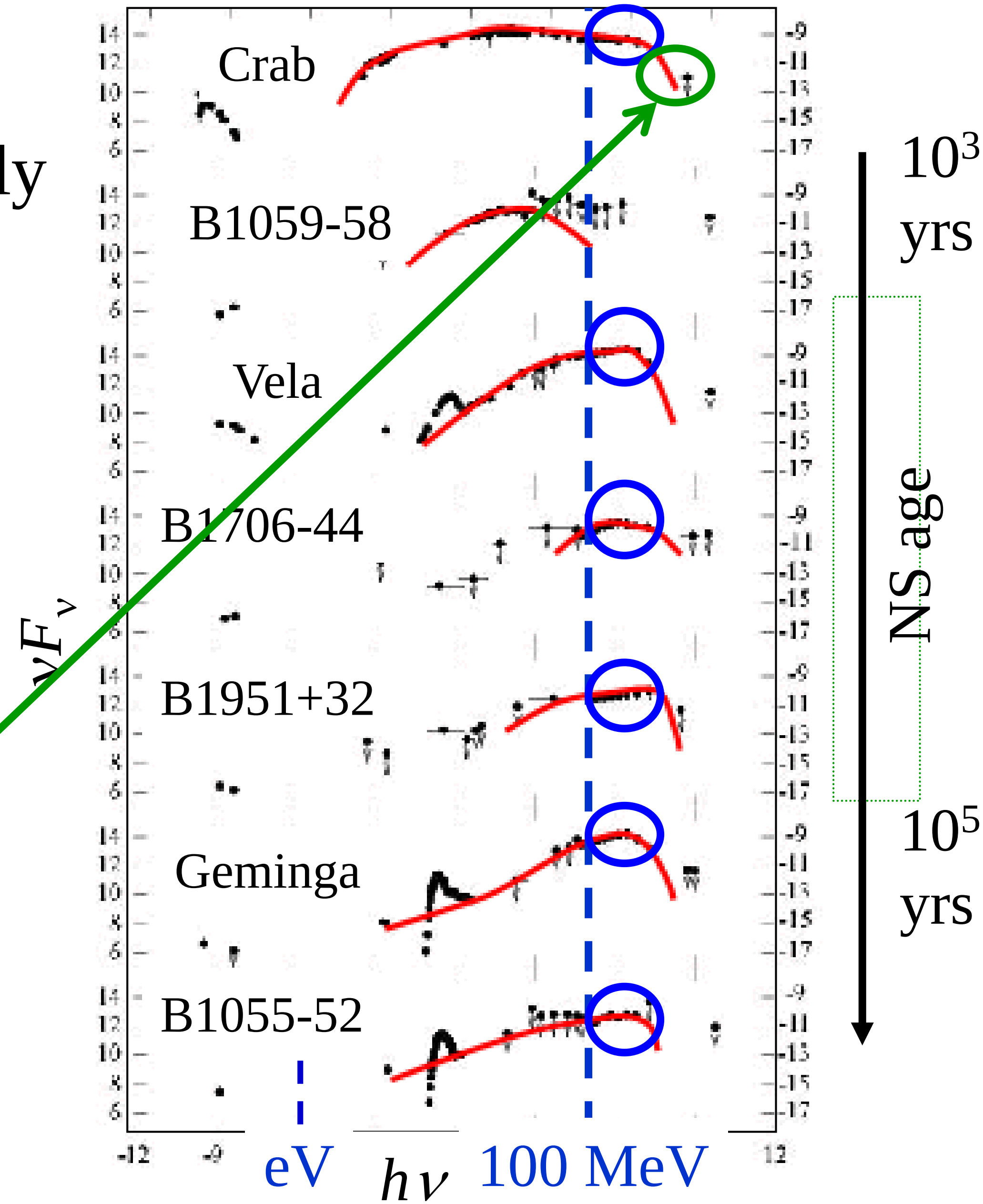

§2 Pulsar Emission Models

Where are such incoherent, high-energy photons emitted from pulsars?

§2 *Pulsar Emission Models*

If copious charges are (somehow) supplied, they realize a force-free magnetosphere, $\boldsymbol{E}\cdot\boldsymbol{B}=0$, and corotate with the magnetosphere under the corotational electric field,

$$\boldsymbol{E}_\perp \equiv -c^{-1}(\boldsymbol{\Omega}\times\boldsymbol{r})\times\boldsymbol{B}.$$

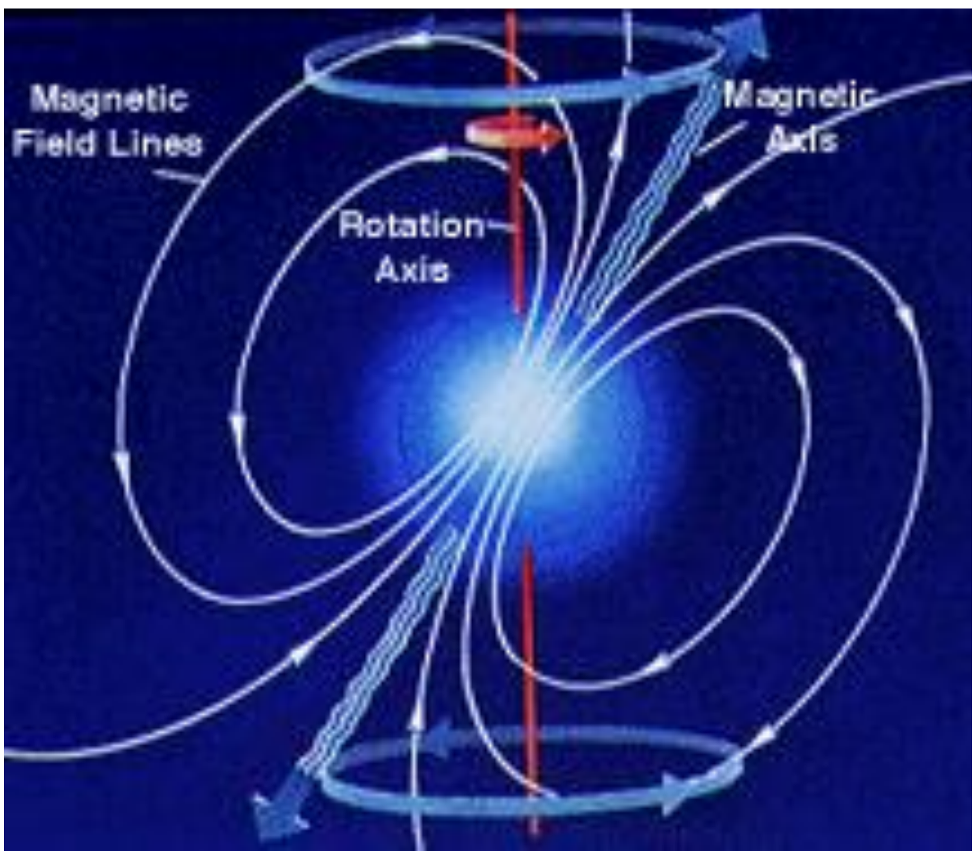

Charges corotate by $\boldsymbol{E}_\perp \times \boldsymbol{B}$ drift,

$$\boldsymbol{v}_\varphi \equiv \boldsymbol{\Omega}\times\boldsymbol{r}.$$

§2 Pulsar Emission Models

If copious charges are (somehow) supplied, they realize a force-free magnetosphere, $\boldsymbol{E}\cdot\boldsymbol{B}=0$, and corotate with the magnetosphere under the corotational electric field,

$$\boldsymbol{E}_{\perp} \equiv -c^{-1}(\boldsymbol{\Omega} \times \boldsymbol{r}) \times \boldsymbol{B}.$$

But $\boldsymbol{E}_{\perp}$ cannot accelerate charged particles.

In $\nabla \cdot \boldsymbol{E} = 4\pi\rho$, we set $\boldsymbol{E} = \boldsymbol{E}_{\perp} + \boldsymbol{E}_{\text{non-corotate}}$, to obtain

$$\nabla \cdot (\boldsymbol{E}_{\perp} + \boldsymbol{E}_{\text{non-corotate}}) = 4\pi\rho,$$

that is,

$$\nabla \cdot \boldsymbol{E}_{\text{non-corotate}} = 4\pi(\rho - \rho_{\text{GJ}}),$$

where $\rho_{\text{GJ}} \equiv \nabla \cdot \boldsymbol{E}_{\perp}/4\pi \sim -\boldsymbol{\Omega} \cdot \boldsymbol{B}/2\pi c.$

If ρ deviates from ρ_{GJ} in some region,

$E_{||} = \boldsymbol{E}_{\text{non-corotate}} \cdot \boldsymbol{B}/\text{B}$ arises around that region.

§2 Pulsar Emission Models

Thus, the problem reduces to …

"Where does the charge deficit ($|\rho| < |\rho_{\mathrm{GJ}}|$) arise?"

But $\boldsymbol{E}_\perp$ cannot accelerate charged particles.

In $\nabla \cdot \boldsymbol{E} = 4\pi\rho$, we set $\boldsymbol{E} = \boldsymbol{E}_\perp + \boldsymbol{E}_{\text{non-corotate}}$, to obtain

$$\nabla \cdot (\boldsymbol{E}_\perp + \boldsymbol{E}_{\text{non-corotate}}) = 4\pi\rho,$$

that is,

$$\nabla \cdot \boldsymbol{E}_{\text{non-corotate}} = 4\pi(\rho - \rho_{\mathrm{GJ}}),$$

where $\rho_{\mathrm{GJ}} \equiv \nabla \cdot \boldsymbol{E}_\perp \sim -\boldsymbol{\Omega} \cdot \boldsymbol{B}/2\pi c$.

If ρ deviates from ρ_{GJ} in some region, $E_{||} = \boldsymbol{E}_{\text{non-corotate}} \cdot \boldsymbol{B}/\mathrm{B}$ arises around that region.

§3 Pulsar Outer gap model

If $E_{||}$ appears in some region, the accelerator (or the gap) boundaries should connect to the force-free magnetosphere outside, i.e., $\rho=\rho_{GJ}$.

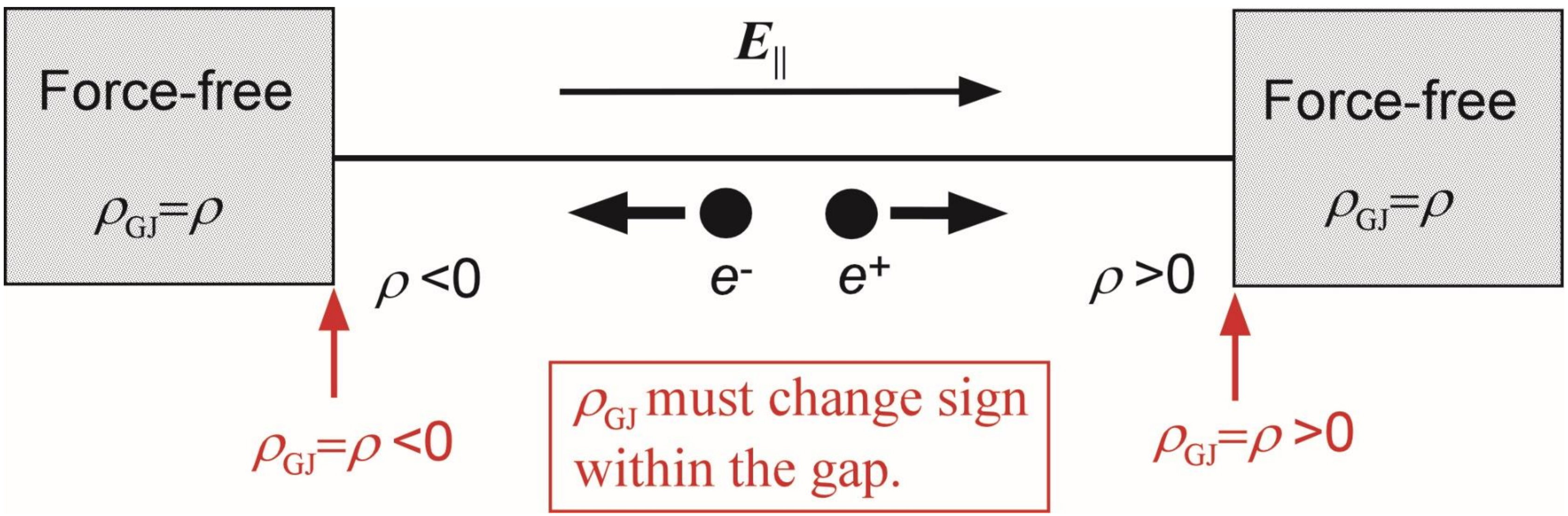

Thus, gap appears across a null charge surface, where $\rho_{GJ}=0$.

§3 *Pulsar Outer gap model*

In pulsar magnetospheres, null-charge surfaces ($\rho_{\rm GJ}$=0) appear due to the global curvature of a dipole ***B*** field.

$$\rho_{\rm GJ} \equiv \nabla \cdot \boldsymbol{E}_{\perp}/4\pi \sim -\boldsymbol{\Omega} \cdot \boldsymbol{B}/2\pi c$$

Null surfaces appear in the higher altitudes (near the light cylinder, ~$10^2\ R_{\rm NS}$), because the open ***B*** lines occupies very small area, on the NS surface.

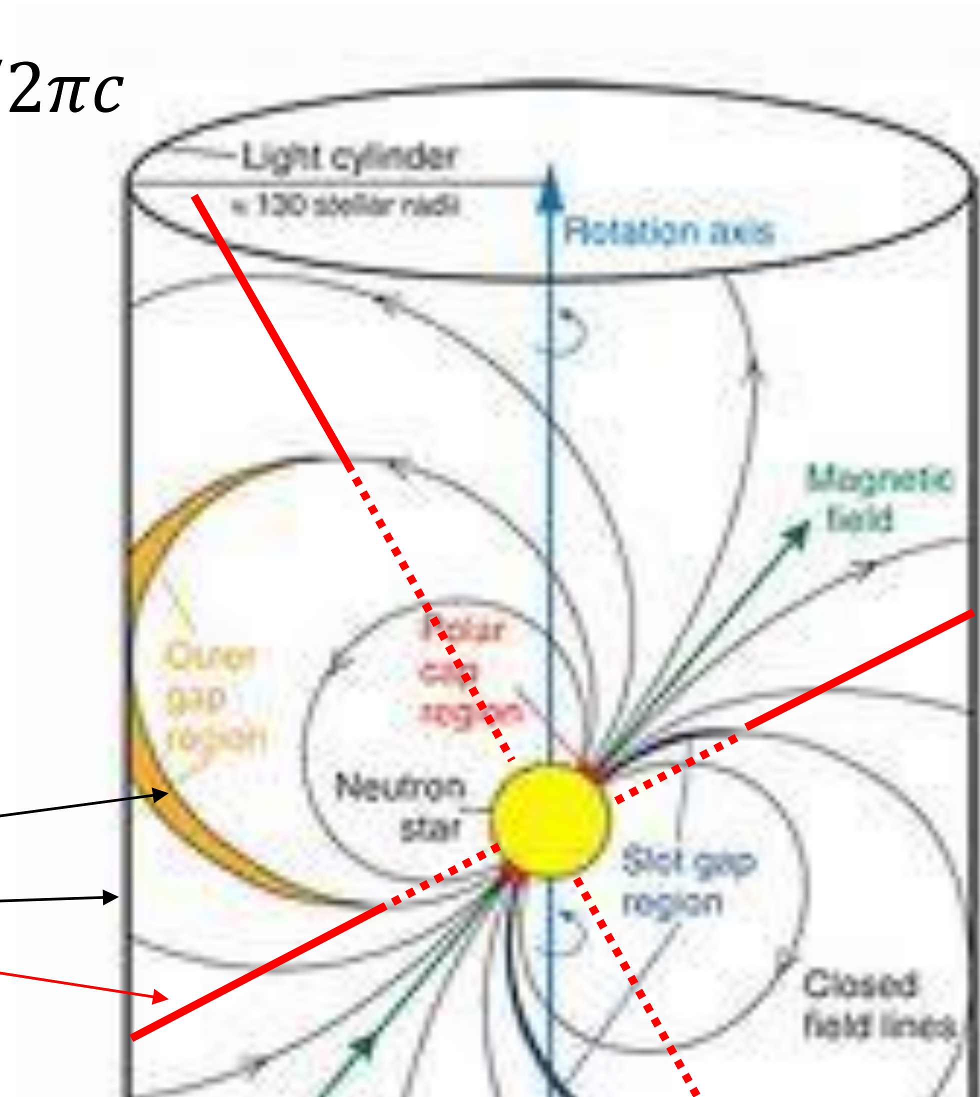

Outer gap

Light cylinder

Null-charge surface

§3 Pulsar Outer gap model

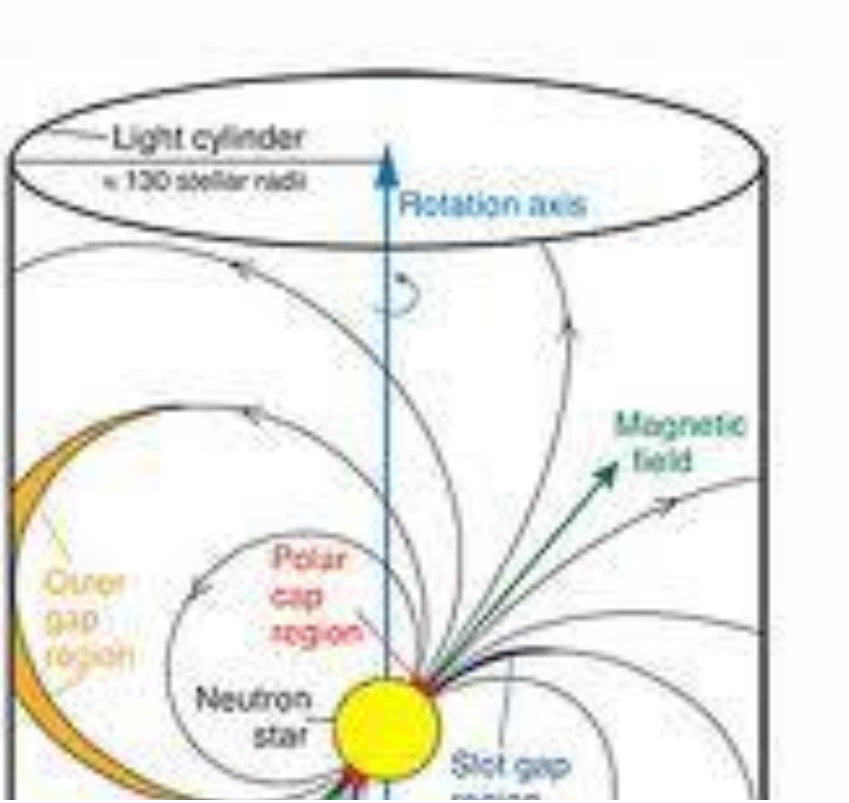

As a model of high-altitude emissions, we investigate the outer gap scenario.

Cheng, Ho, Ruderman (1986, ApJ 300, 500)

Emission altitude

~ light cylinder

⟶ hollow cone emission

($\Delta\Omega$ > 1 ster)

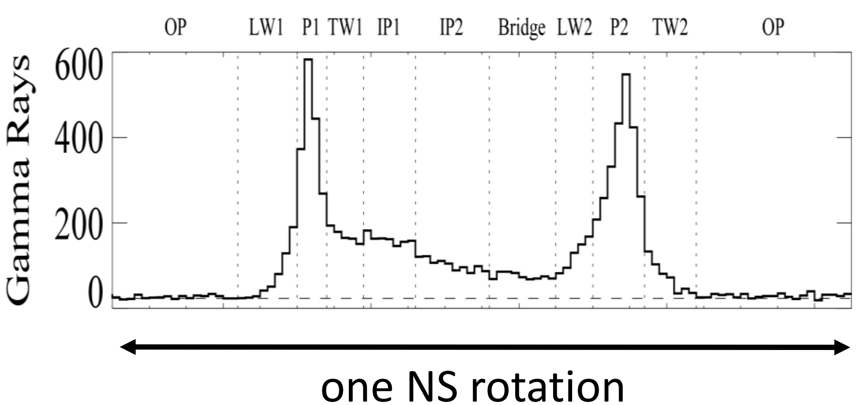

Successfully explained wide-separated double peaks.

OG model became promising.

§3 Outer-gap Model: Formalism

I quantify the classic OG model by solving the pair-production cascade in a rotating NS magnetosphere:

$e^{\pm}$'s are accelerated by $E_{||}$

↓

Relativistic e^+/e^- emit γ-rays via synchro-curvature, and IC processes

↓

γ-rays collide with soft photons/B to materialize as pairs in the accelerator

§3 Outer-gap Model: Formalism

Poisson equation for electrostatic potential ψ :

$$-\nabla^2\psi = -\frac{\partial^2\psi}{\partial x^2} - \frac{\partial^2\psi}{\partial y^2} - \frac{\partial^2\psi}{\partial z^2} = 4\pi(\rho - \rho_{\rm GJ}) \ ,$$

where

$$E_{\|} \equiv -\frac{\partial\psi}{\partial x} \ , \ \rho_{\rm GJ} \equiv -\frac{\mathbf{\Omega}\bullet\mathbf{B}}{2\pi c},$$

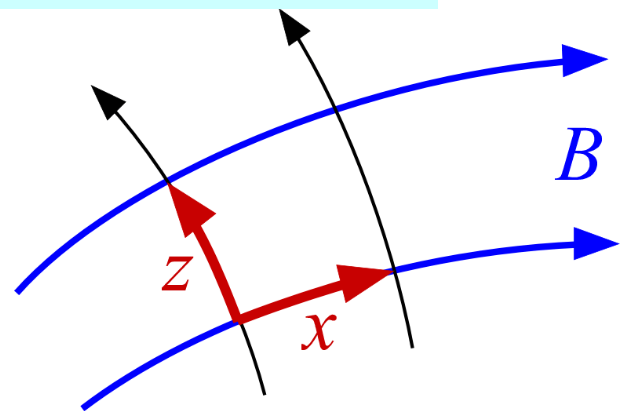

$$\rho(\mathbf{x}) \equiv e\int_1^\infty d\gamma \int_0^\pi d\chi \left[N_+(\mathbf{x},\gamma,\chi) - N_-(\mathbf{x},\gamma,\chi)\right] + \rho_{\rm ion}(\mathbf{x}),$$

$$\mathbf{x} = (x, y, z) \ .$$

N_+/N_-: distrib. func. of e^+/e^-

γ : Lorentz factor of e^+/e^-

χ : pitch angle of e^+/e^-

§3 Outer-gap Model: Formalism

Assuming $\partial_t + \Omega \partial_\phi = 0$, we solve the $e^{\pm}$'s Boltzmann eqs.

$$\frac{\partial N_\pm}{\partial t} + \vec{v} \cdot \nabla N_\pm + \left(e\vec{E}_\parallel + \frac{\vec{v}}{c} \times \vec{B} \right) \cdot \frac{\partial N_\pm}{\partial \vec{p}} = S_{IC} + S_{SC} + \int \alpha_\nu d\nu \int \frac{I_\nu}{h\nu} d\omega$$

together with the radiative transfer equation,

$$\frac{dI_\nu}{dl} = -\alpha_\nu I_\nu + j_\nu$$

$N_\pm$: positronic/electronic spatial # density,
$E_\parallel$: mangnetic-field-aligned electric field,
$S_{\rm IC}$: ICS re-distribution function, $d\omega$: solid angle element,
I_ν: specific intensity, l : path length along the ray
α_ν: absorption coefficient, j_ν: emission coefficient

§4 OG model: the Crab pulsar

Next, we apply the scheme to the Crab pulsar.

Recent force-free, MHD, and PIC simulations suggest that ***B*** field approaches a **split monopole** (Michael'74) near and beyond the light cylinder.

Thus, we consider

$$\boxed{\begin{aligned} \boldsymbol{B} &= \text{vacuum, rotating dipole } \boldsymbol{B} \\ &\quad + b \times \text{ split-monopole } \boldsymbol{B} \end{aligned}}$$

b=0: pure dipole

b=1: $B_{\text{dipole}}=B_{\text{monopole}}$ @ LC

§4 OG model: the Crab pulsar

3-D distribution of the particle accelerator (i.e., high-energy emission zone) solved from the Poisson eq.:

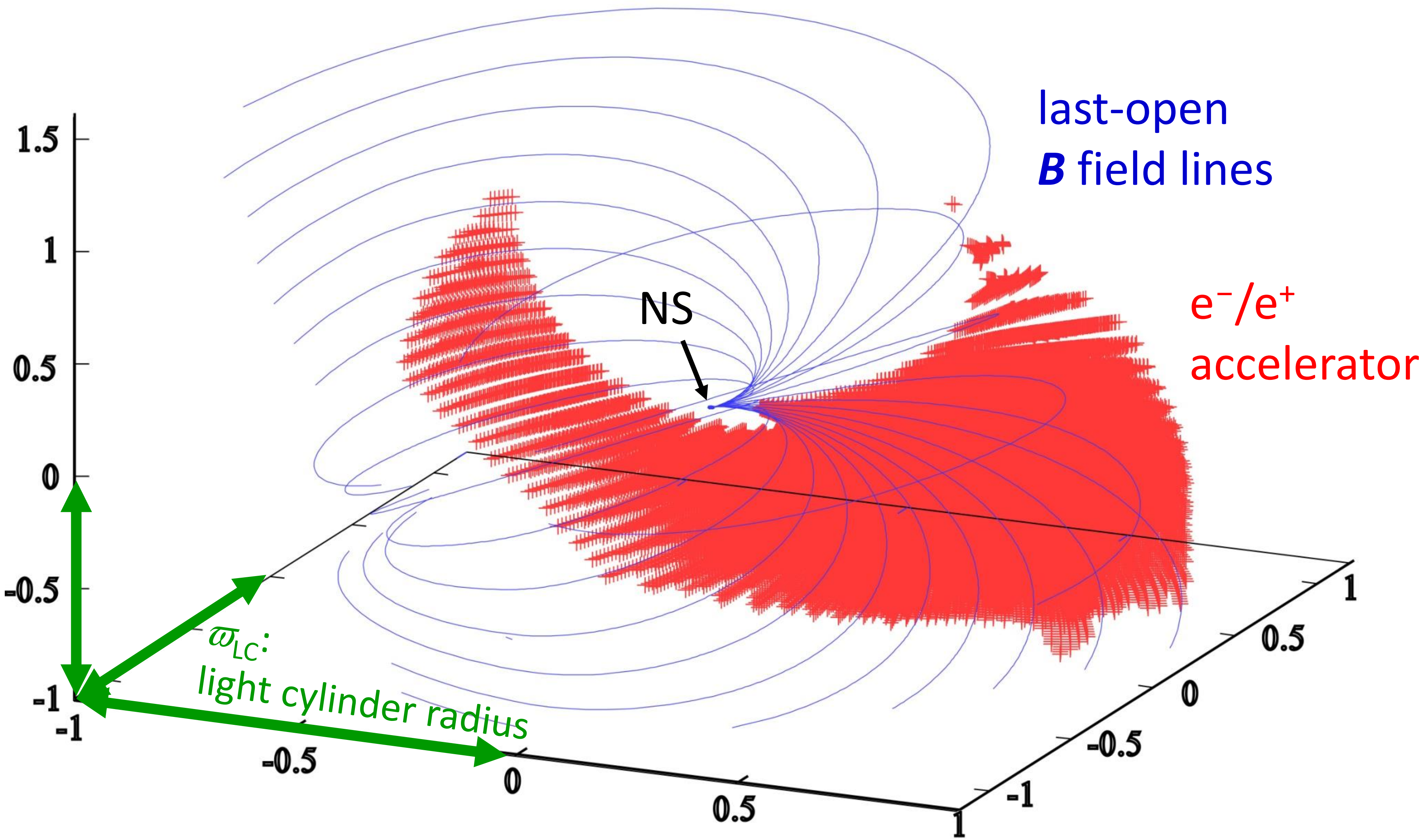

§4 OG model: the Crab pulsar

$E_{\parallel}$ is heavily screened by the produced pairs.

$\rightarrow$ Outward flux » Inward flux (KH '15, ApJ 798, L40).

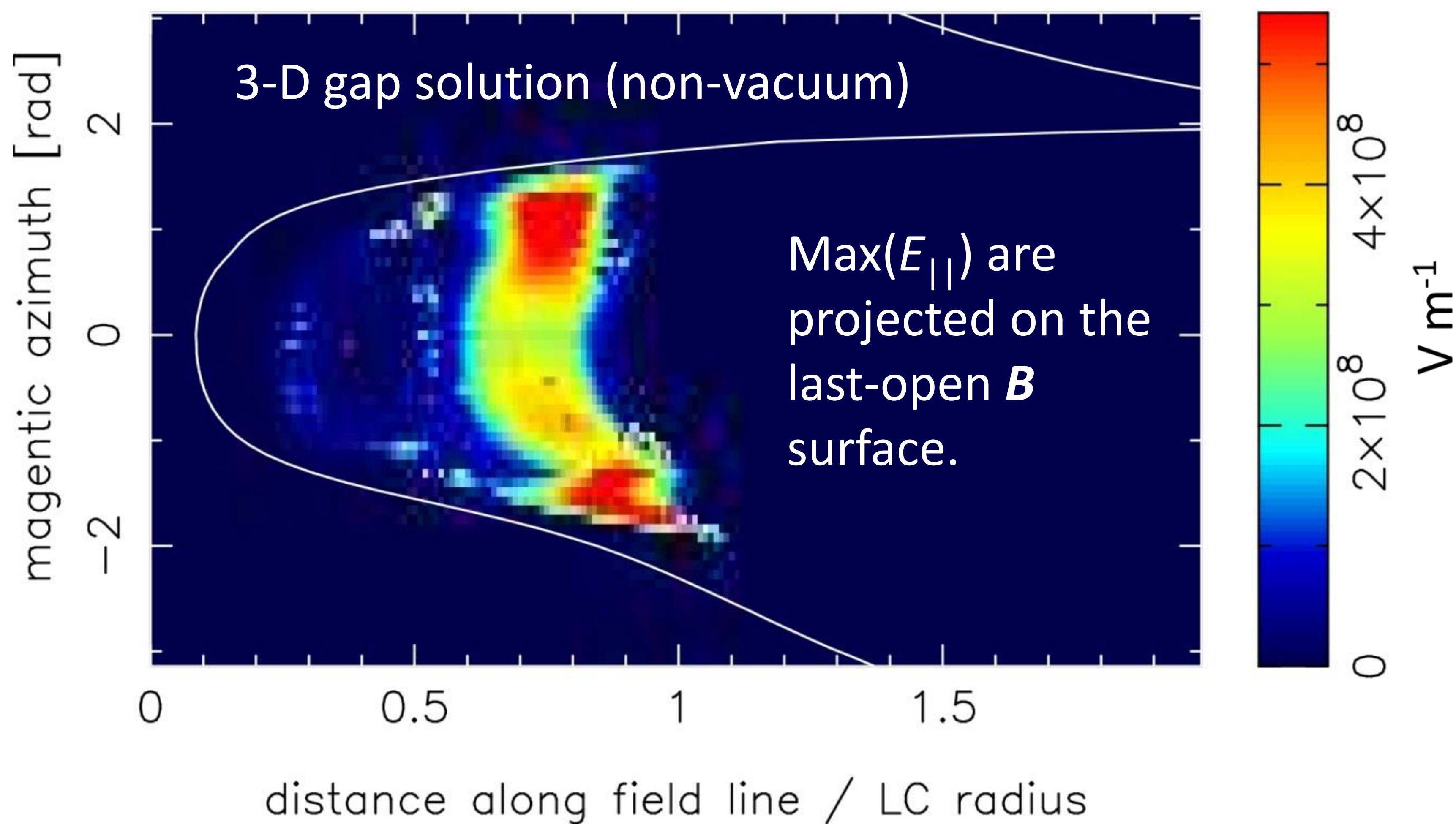

§4 OG model: the Crab pulsar

The resultant γ-ray light curves changes as a function of the observer's viewing angles:

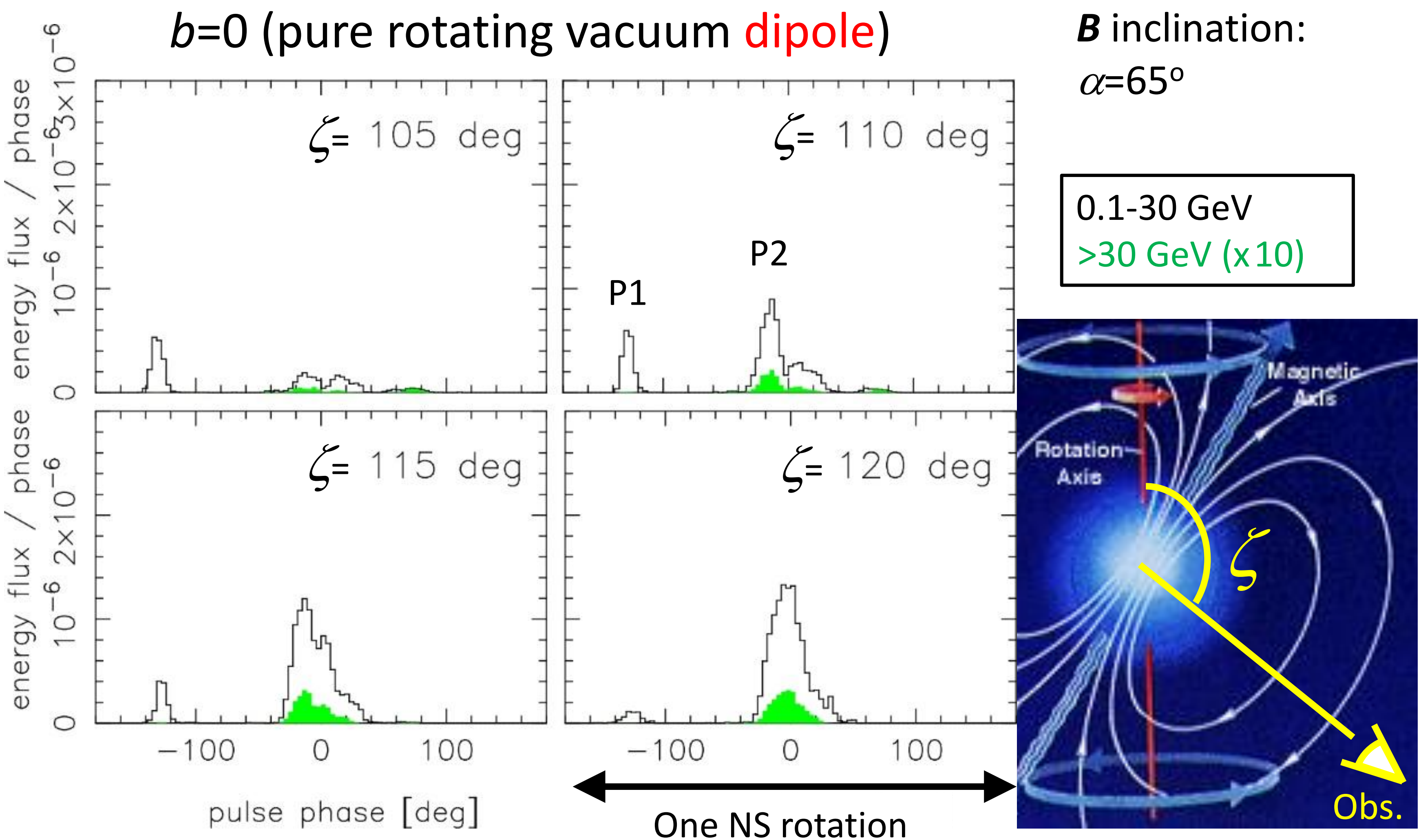

§4 OG model: the Crab pulsar

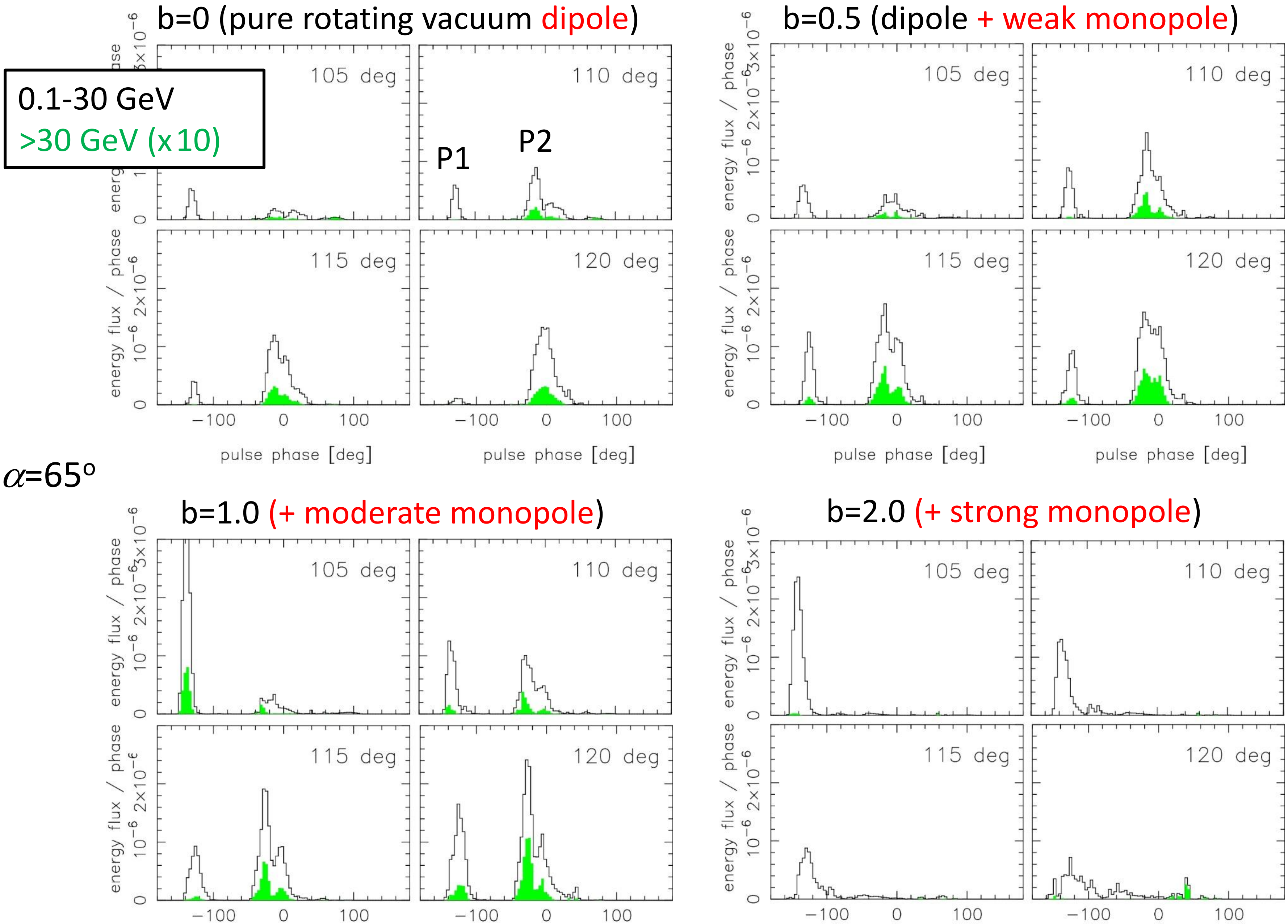

§4 OG model: the Crab pulsar

b=0 (pure rotating vacuum dipole)

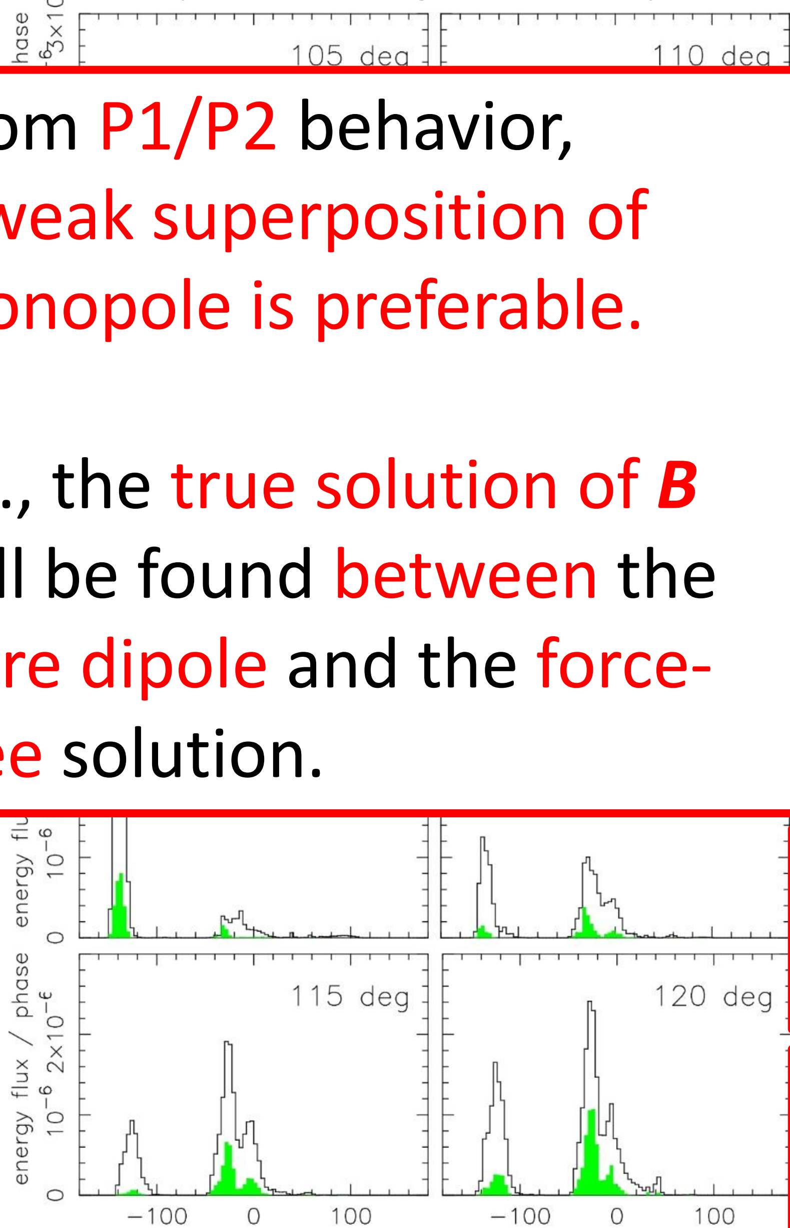

From P1/P2 behavior,
a weak superposition of monopole is preferable.

I.e., the true solution of ***B*** will be found between the pure dipole and the force-free solution.

b=0.5 (dipole + weak monopole)

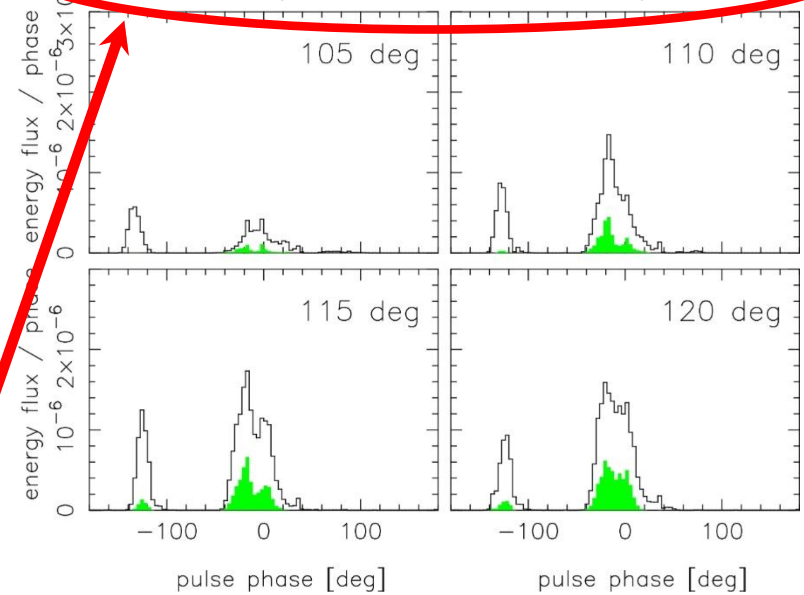

b=2.0 (+ strong monopole)

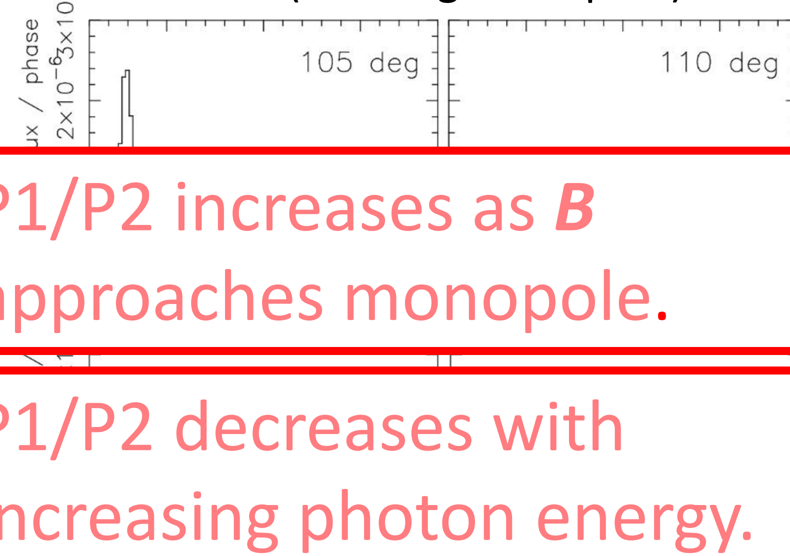

P1/P2 increases as ***B*** approaches monopole.

P1/P2 decreases with increasing photon energy.

§4 OG model: the Crab pulsar

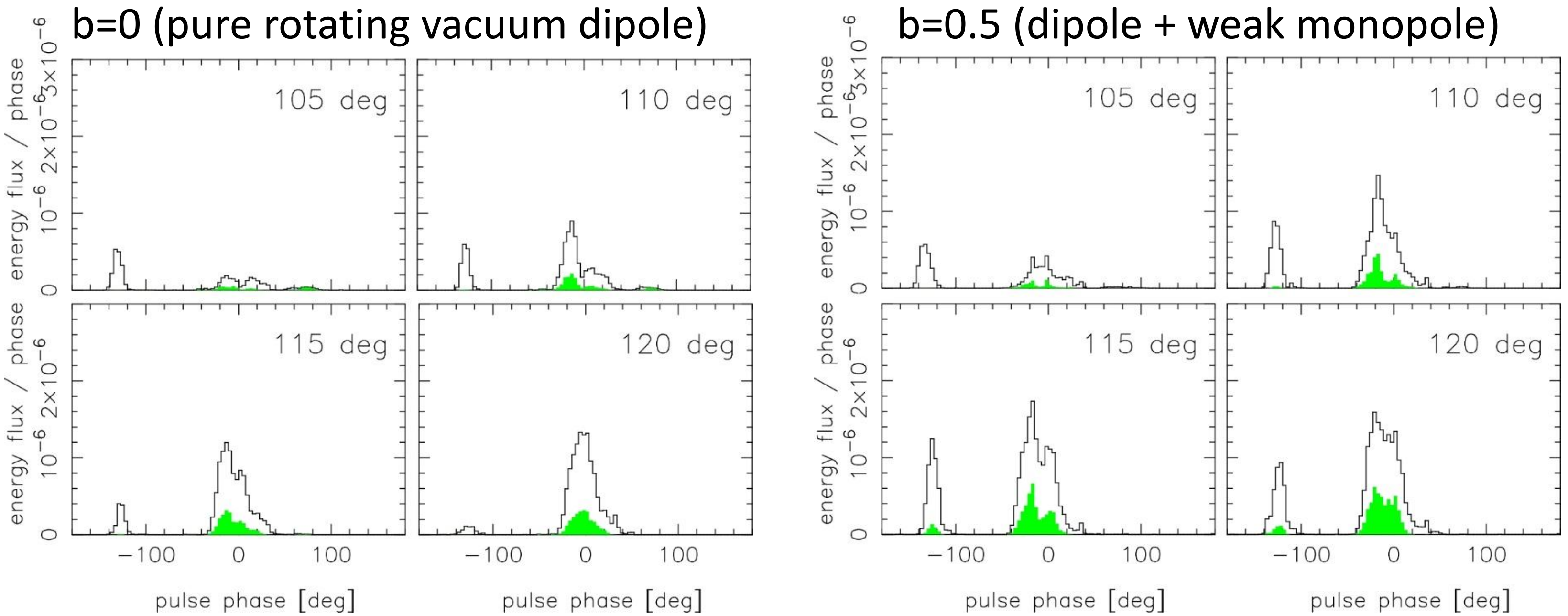

For very young pulsars like Crab, P2 spectrum gets harder than P1, because γγ collision angles are small in TS due to the caustic (aberration+time-of-flight delay) effect.

Cf. In general, P2 curvature specrum is harder than P1, because R_c is greater in TS. (KH ApJ 733, L49, 2011)

§4 OG model: the Crab pulsar

Phase-resolved spectrum (Crab, b=0.5, α=65°, ζ=118°)

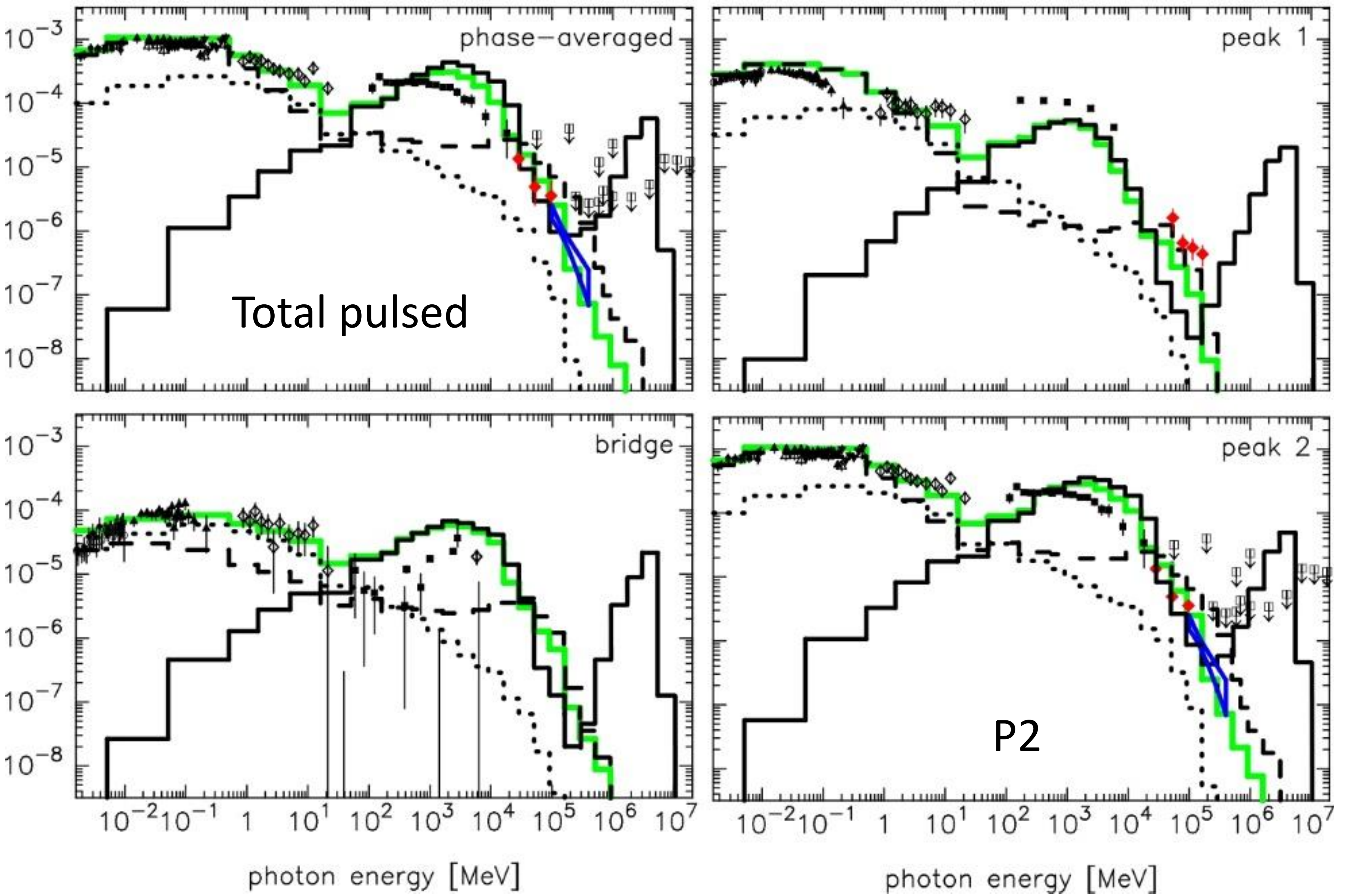

§4 OG model: the Crab pulsar

Viewing angle dependence: ζ=95^o for b=0 & α=60^o

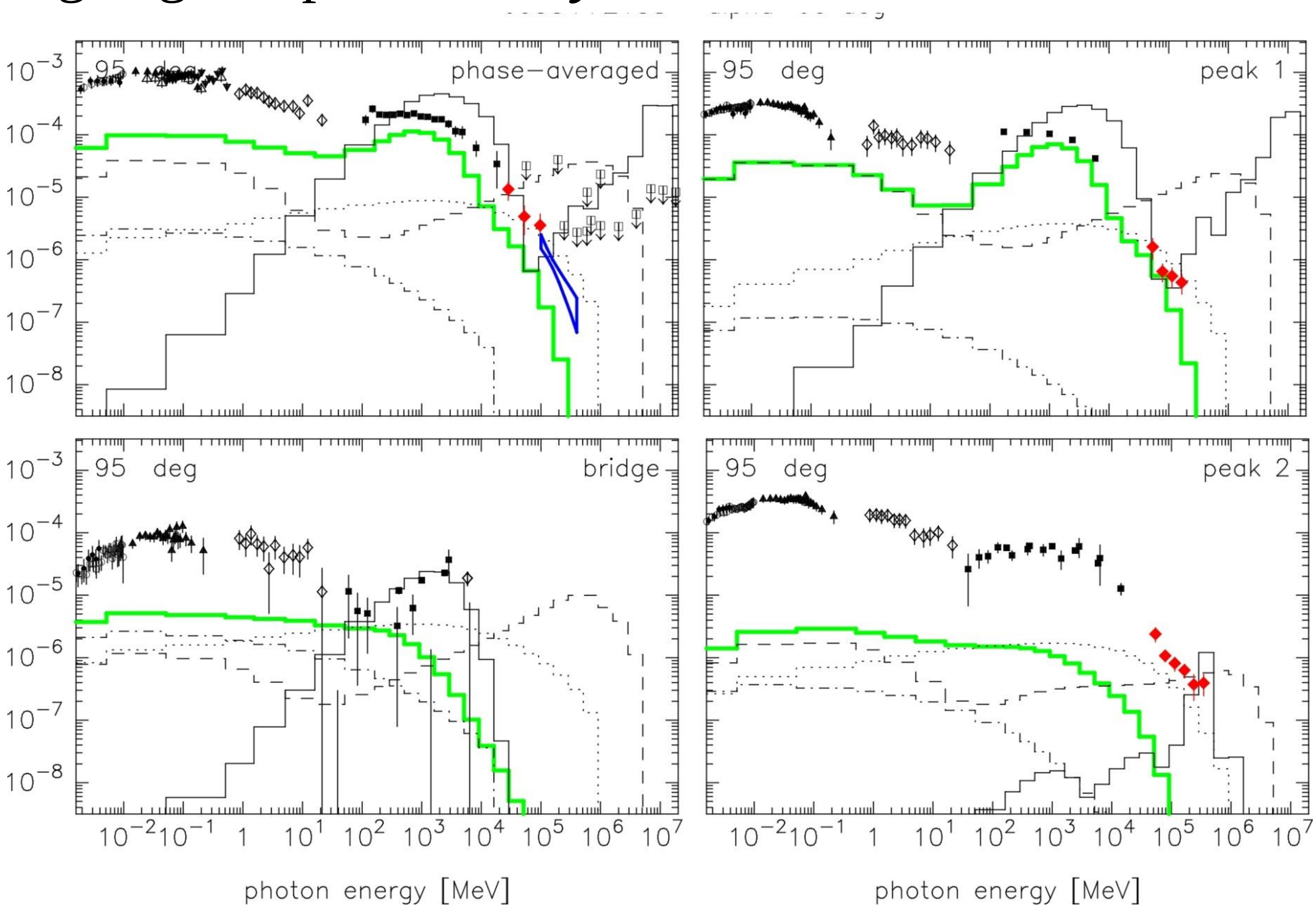

§4 OG model: the Crab pulsar

Viewing angle dependence: $\zeta=100^{\circ}$ for $b=0$ & $\alpha=60^{\circ}$

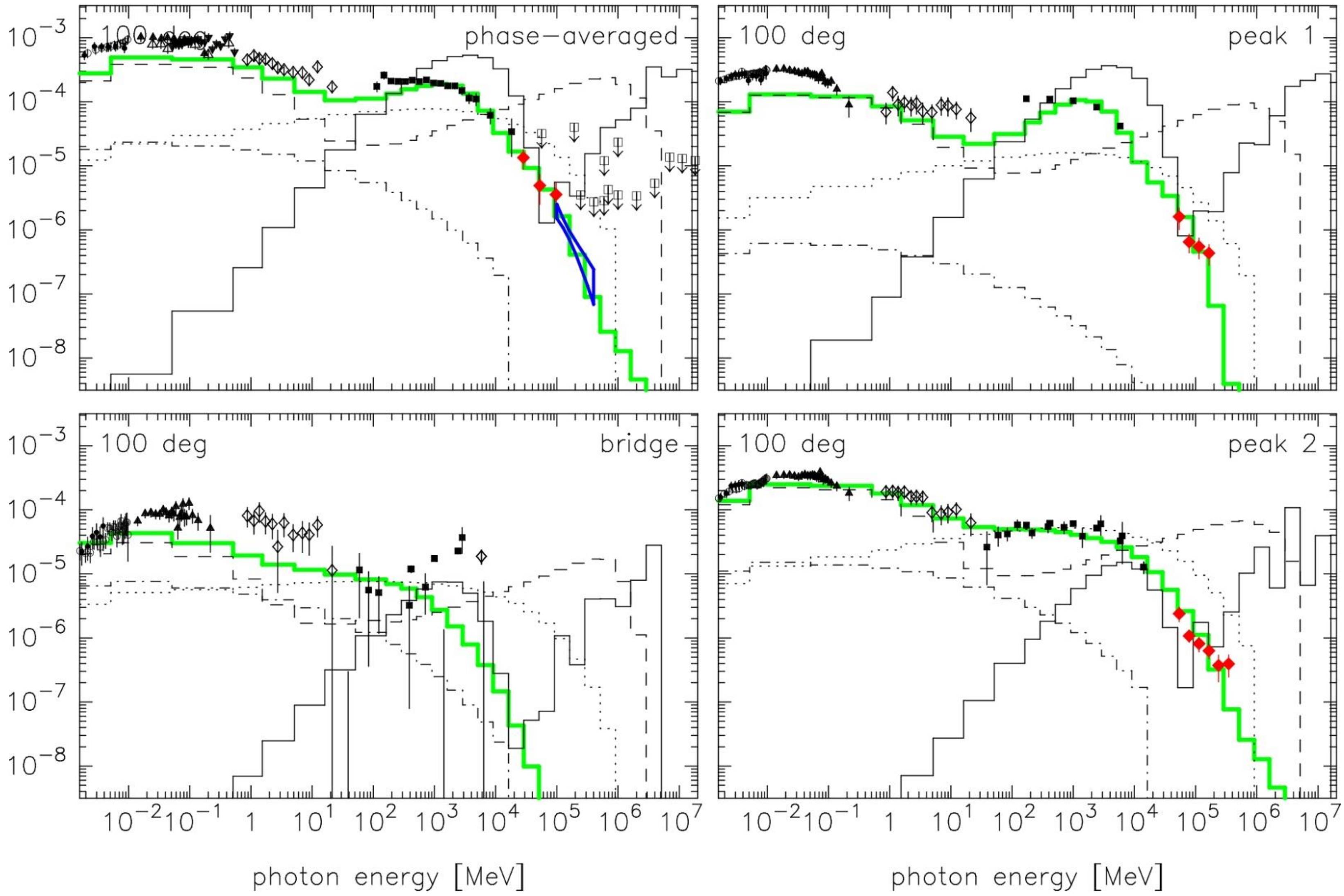

§4 OG model: the Crab pulsar

Viewing angle dependence: ζ=105° for b=0 & α=60°

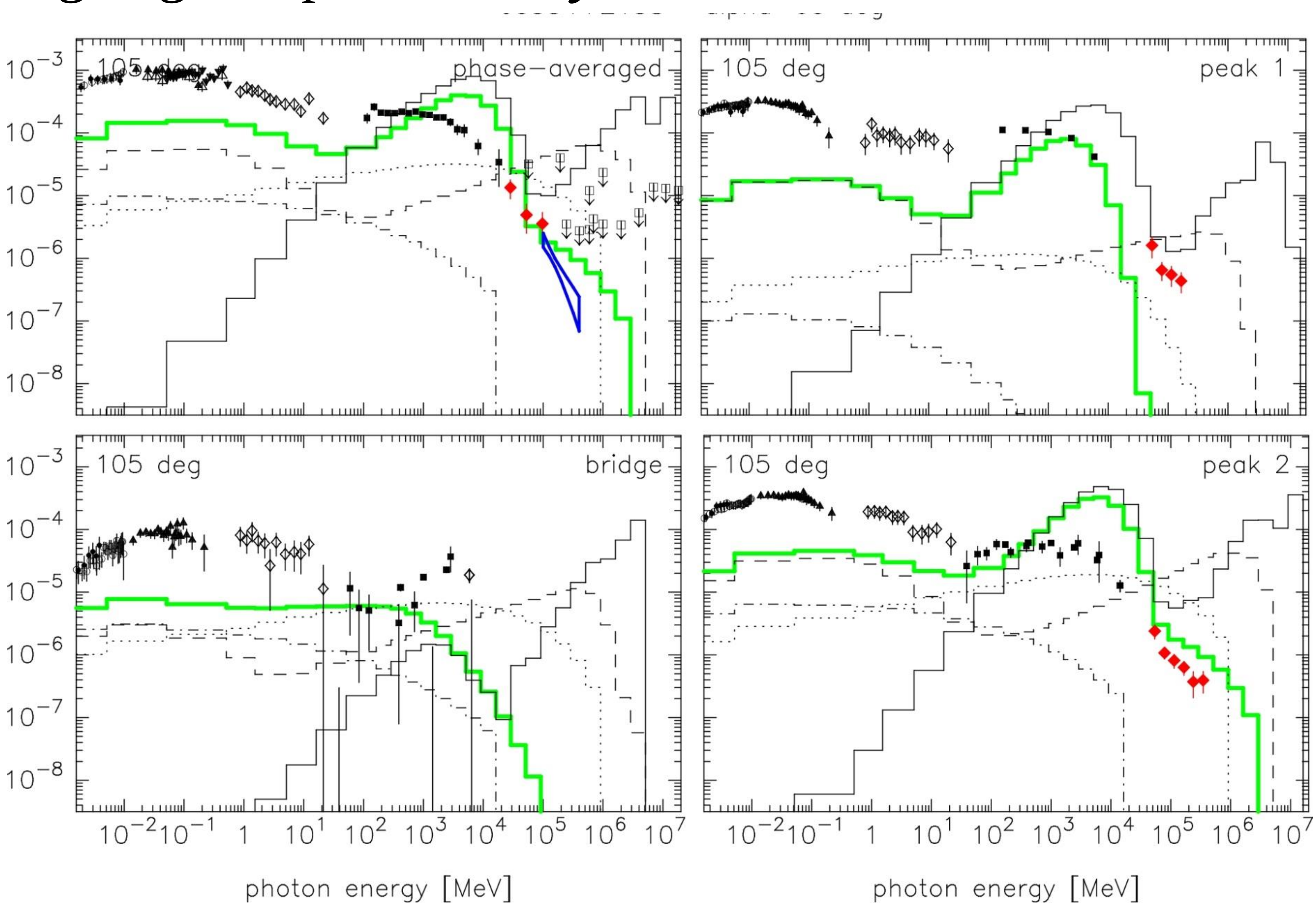

§4 OG model: the Crab pulsar

Viewing angle dependence: ζ=105° for b=0 & α=60°

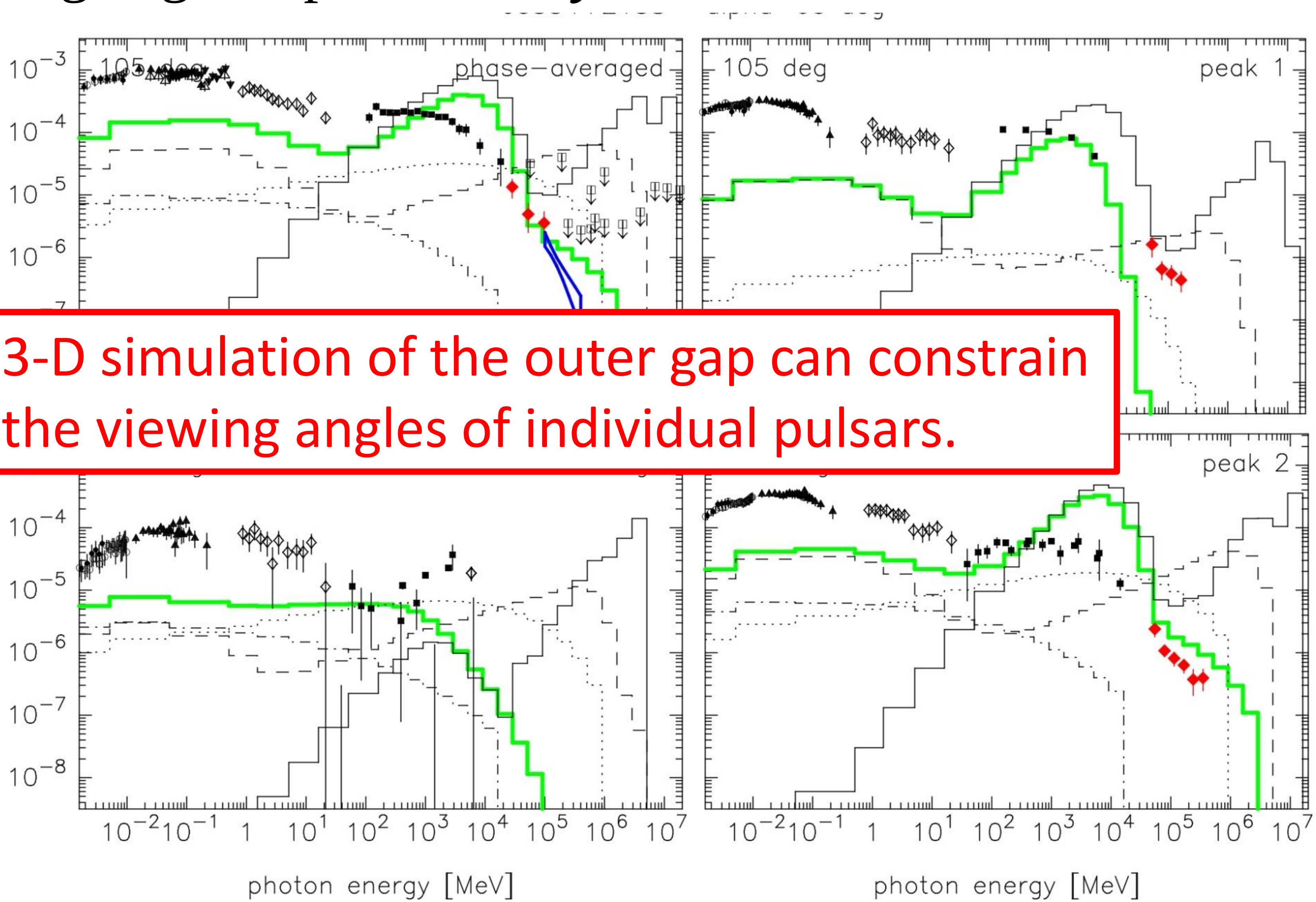

3-D simulation of the outer gap can constrain the viewing angles of individual pulsars.

§5 BH gap model

Same method can be applied to BH magnetospheres.

The BH gap model itself is applicable to arbitrary BH mass (from stellar-mass to supermassive), spin, and accretion rate (from LLAGN to quasars)

Beskin + (1992, Soviet Ast. 36, 642)
KH & Okamoto (1998, ApJ 497, 653)

We present a new method to quantify the previous BH models (Levinson & Rieger 2011, ApJ 730, 123; Broderick & Tchekhovskoy 2015, ApJ 809, 97).

Today, as an example, we apply the BH gap model to IC310. KH & Pu (2015, ApJ, submitted)

§5 BH gap model

A possible target: IC310

BH lightning due to particle acceleration @ horizon scale

(Science 346, 1080-1084, MAGIC collaboration 2014)

MAGIC observed radio galaxy IC 310 (S0, z =0.0189) on Nov 12-13, 2012. M-σ rel.→ $M=(1\sim7)\times10^8\, M_\odot$, Δt_{BH} = 8~57 min.

Extraordinary outburst was detected above 300 GeV.

Conservative estimate of the shortest variability, Δt_{obs}=4.8 min < (.08-.6)Δt_{BH}

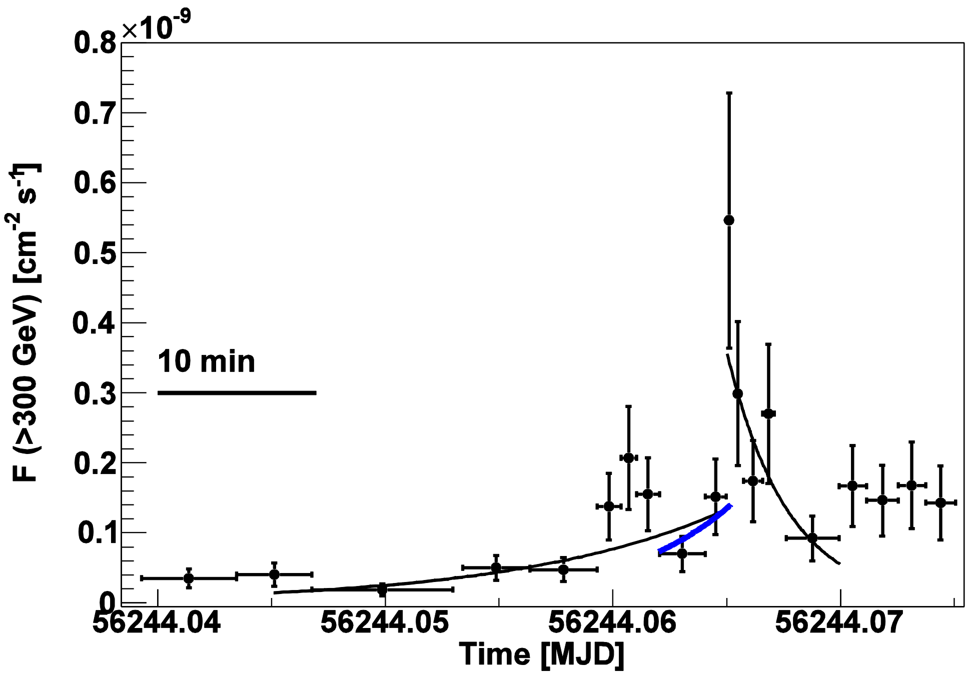

§5 BH gap model

BH lightning due to particle acceleration @ horizon scale

(Science 346, 1080-1084, MAGIC collaboration 2014)

If the initial perturbation originates in the AGN-rest frame, the variability takes place at sub-horizon scale.

Mrk 501 & PKS 2155-304 show VHE variabilities with flux doubling times scales, $\Delta t_{\mathrm{obs}} \sim 2$ min « Δt_{BH}. (~70-80 min.)

(Albert + 2007, ApJ 685, L23; Abramowski + 2012, ApJ 746, 151)

Imagine a perturbation initiating in the AGN-rest frame with variation time scale Δt_{AGN}.

The perturbation enters into the jet with time scale $\Gamma \Delta t_{\mathrm{AGN}}$.

We detect variation $\Delta t_{\mathrm{obs}} = (1+z)\,(\Gamma/\delta)\,\Delta t_{\mathrm{AGN}} \sim \Delta t_{\mathrm{AGN}}$.

Since $\Gamma \sim \delta$, Lorentz factors cancel out in the observer's frame.

→ Δt_{obs} « Δt_{BH} indicates variations at sub-horizon scales.

§ 5 BH gap model

To interpret the sub-horizon phenomena, we apply the pulsar outer-gap model to the BH magnetosphere of IC 310.

GR Goldreich-Julian charge density:

$$\rho_{\rm GJ} \equiv -\frac{1}{4\pi}\nabla\bullet\left(\frac{\Omega-\omega}{2\pi\alpha c}\nabla\Psi\right)$$

Ω: angular frequency of ***B*** field

ω: angular frequency of space-time dragging

α: redshift factor (or the lapse function)

Ψ: magnetic flux function, A_ϕ. describes

$$\mathbf{B}_p = -\frac{e_\phi \times \nabla\Psi}{2\pi\varpi}, \quad \mathbf{E}_p = -\frac{\Omega-\omega}{2\pi\alpha c}\nabla\Psi$$

In BH magnetosphere, null surface is formed by space-time dragging near the horizon, close to the Ω=ω surface.

§ 5 BH gap model

Distribution of null surface ($\rho_{GJ}=0$ due to frame dragging).

KH & Pu 2015, submitted to ApJ

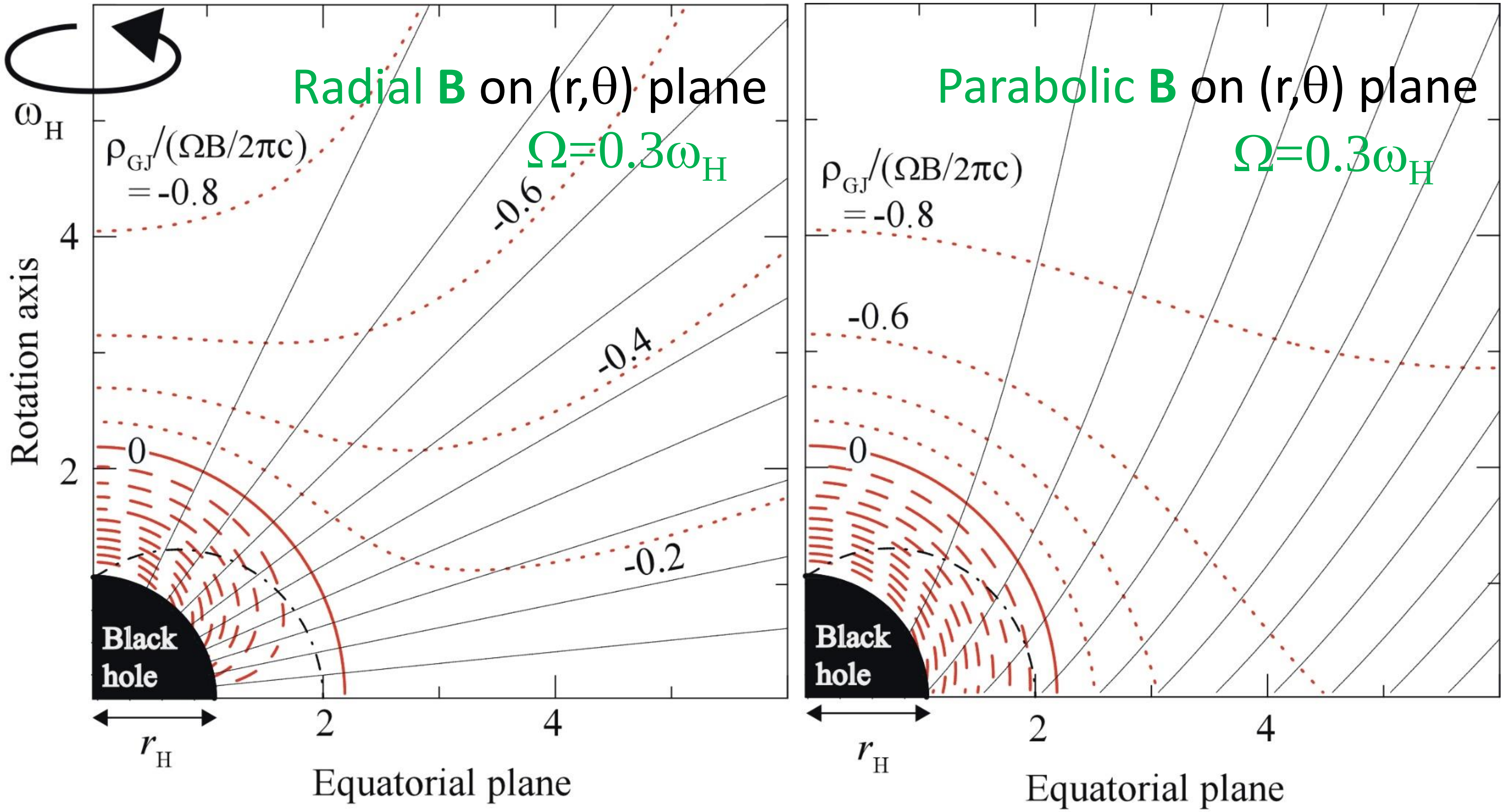

§ 5 BH gap model

Gap exits as a solution of the set of Poisson eq. for Ψ and $e^{\pm}$ & γ Boltzmann eqs.

$E_{\parallel}$ arises along $\boldsymbol{B}$.

Frame dragging determines ρ_{GJ}. Thus, $\rho_{GJ}(r,\theta)$ and hence the solution little depends on $\boldsymbol{B}\,(r,\theta)$.

We thus assume radial $\boldsymbol{B}$ on poloidal plane.

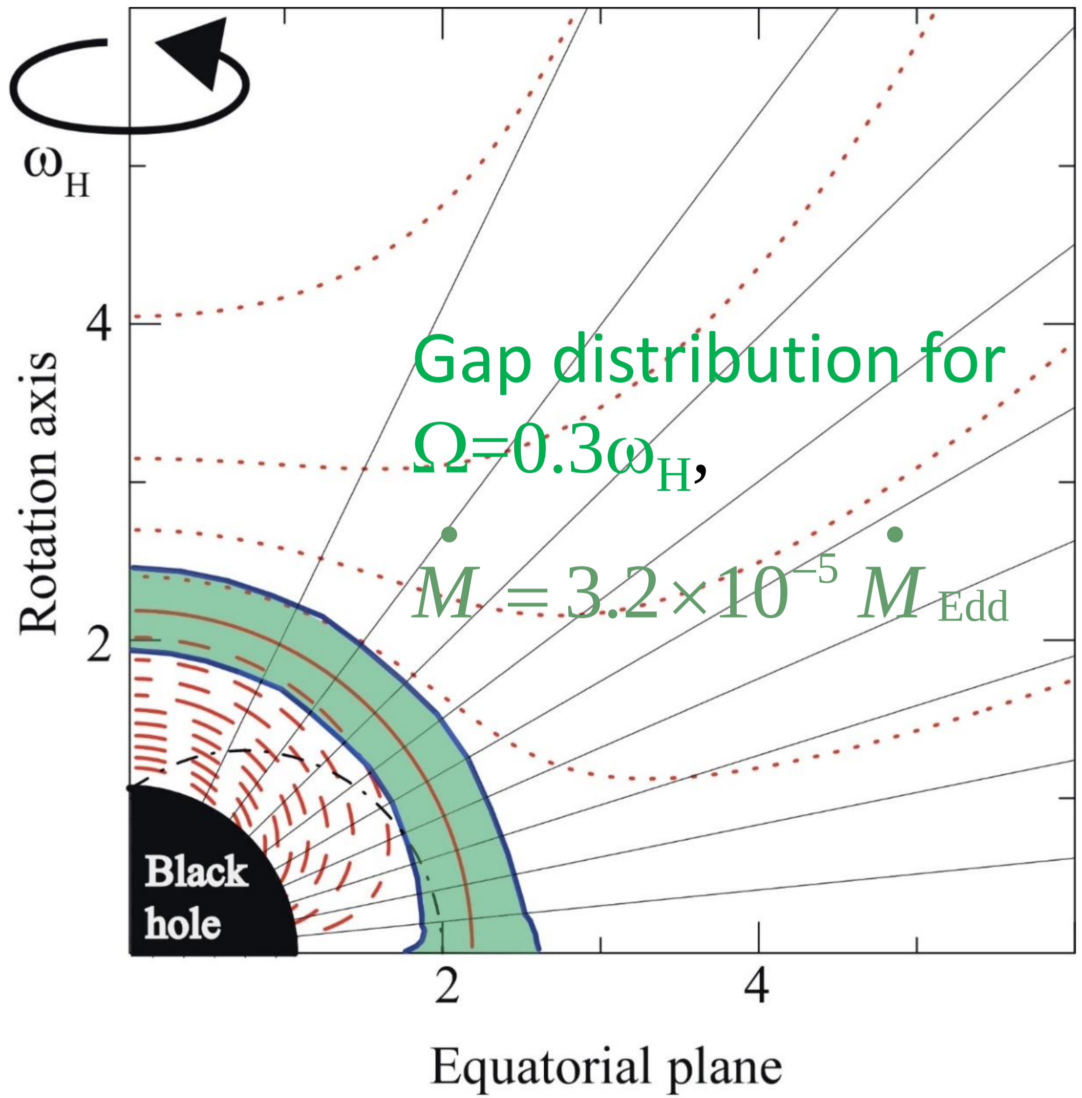

KH & Pu 2015, submitted to ApJ

§ 5 BH gap model

Poisson eq: $\nabla \cdot E_{\|} = 4\pi(\rho - \rho_{GJ})$ KH & Pu 2015, submitted to ApJ

Along ***B***,
$\rho \neq \rho_{GJ}$,
leading to non-vanishing $E_{\|}$.

Example of
$E_{\|}(s)$ at $\theta = 15^{o}$
(polar funnel).

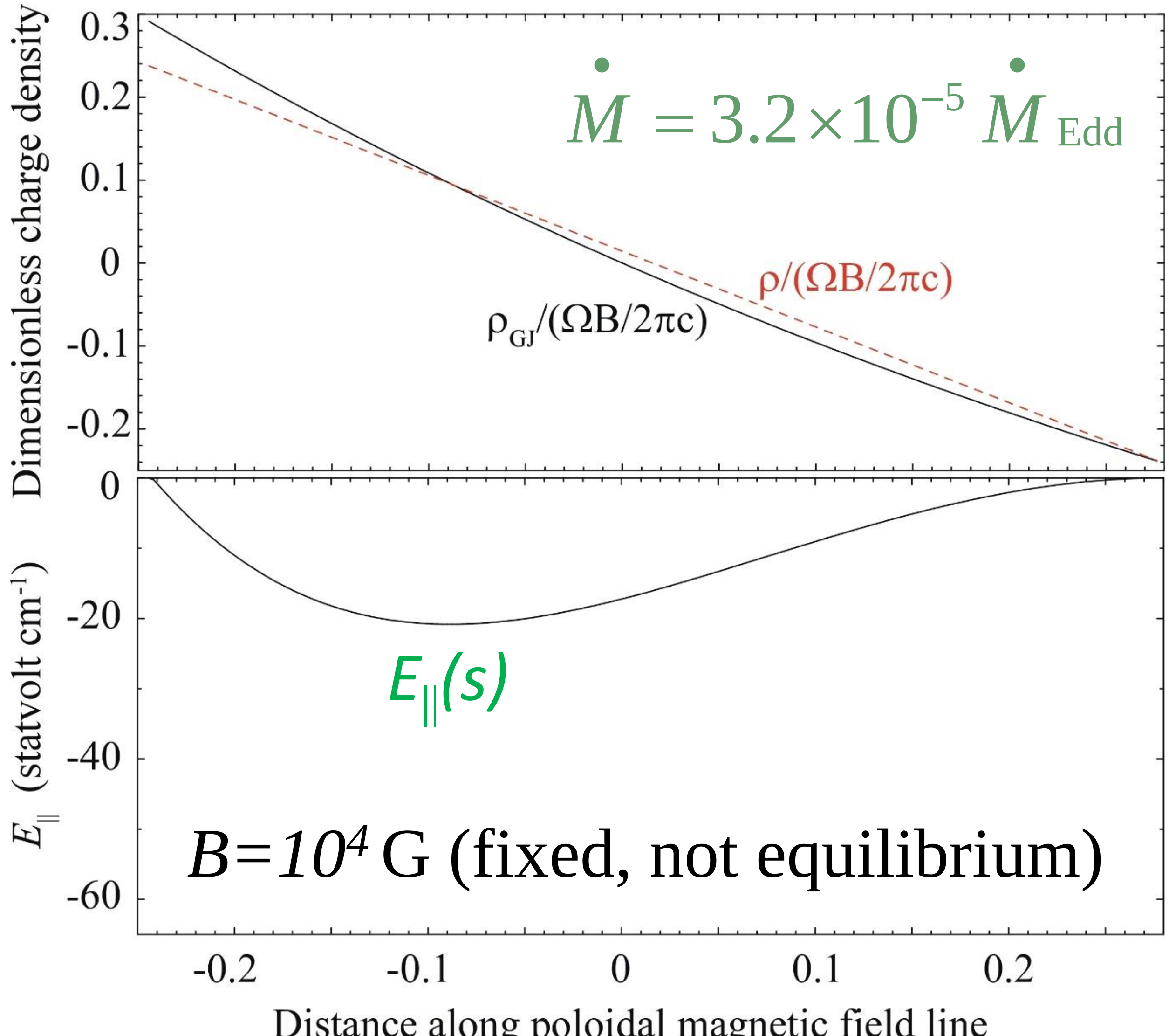

§ 5 BH gap model: Results

w increases with decreasing $\dot{M}/\dot{M}_{\rm Edd}$.

Since $L_{\rm gap} \propto w^4$, the gap becomes most luminous when the inner boundary almost touches down the horizon.

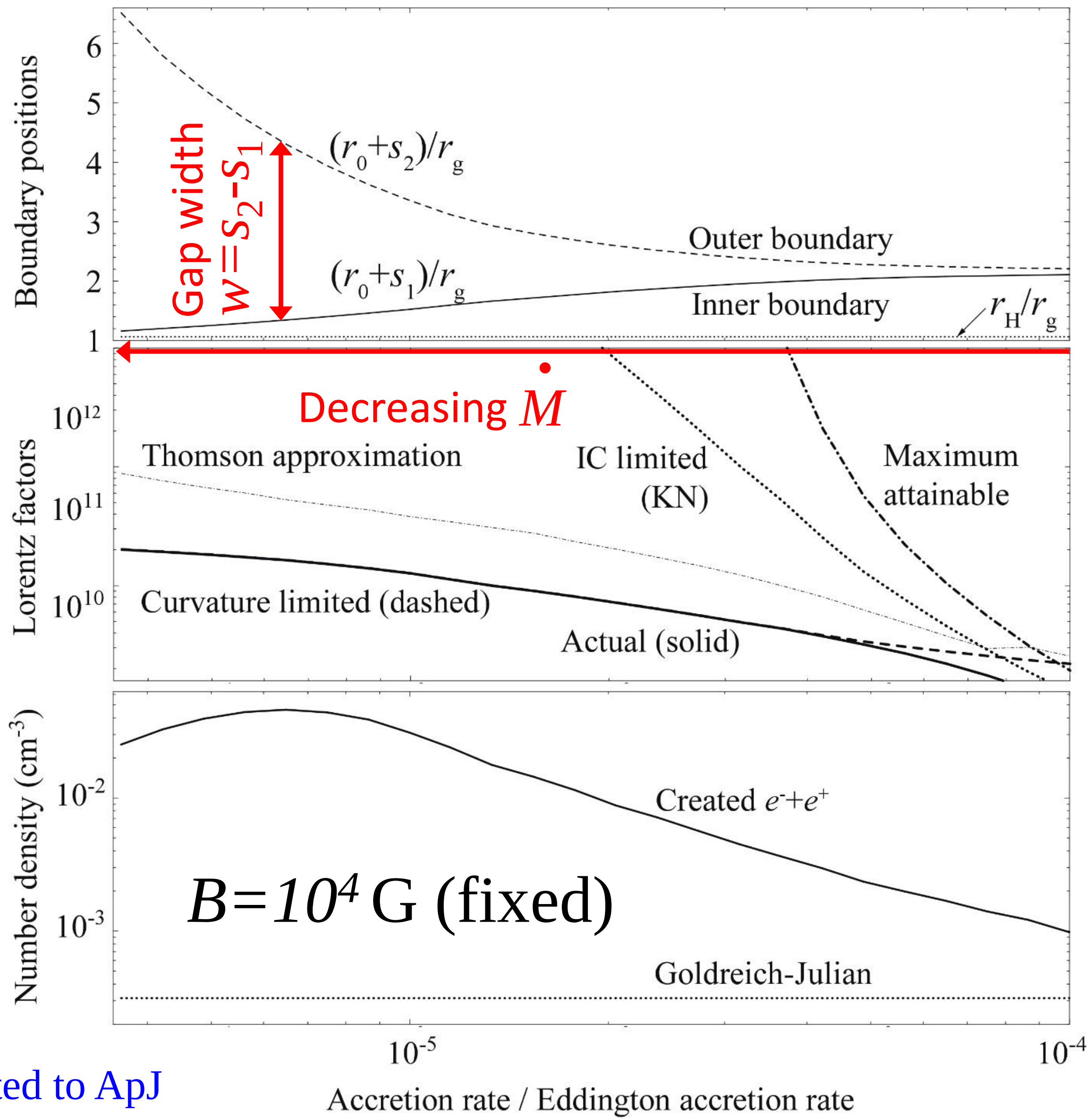

KH & Pu 2015, submitted to ApJ

§ 5 BH gap model

Large curvature radius, $R_c = 10r$.

KH & Pu 2015, submitted to ApJ

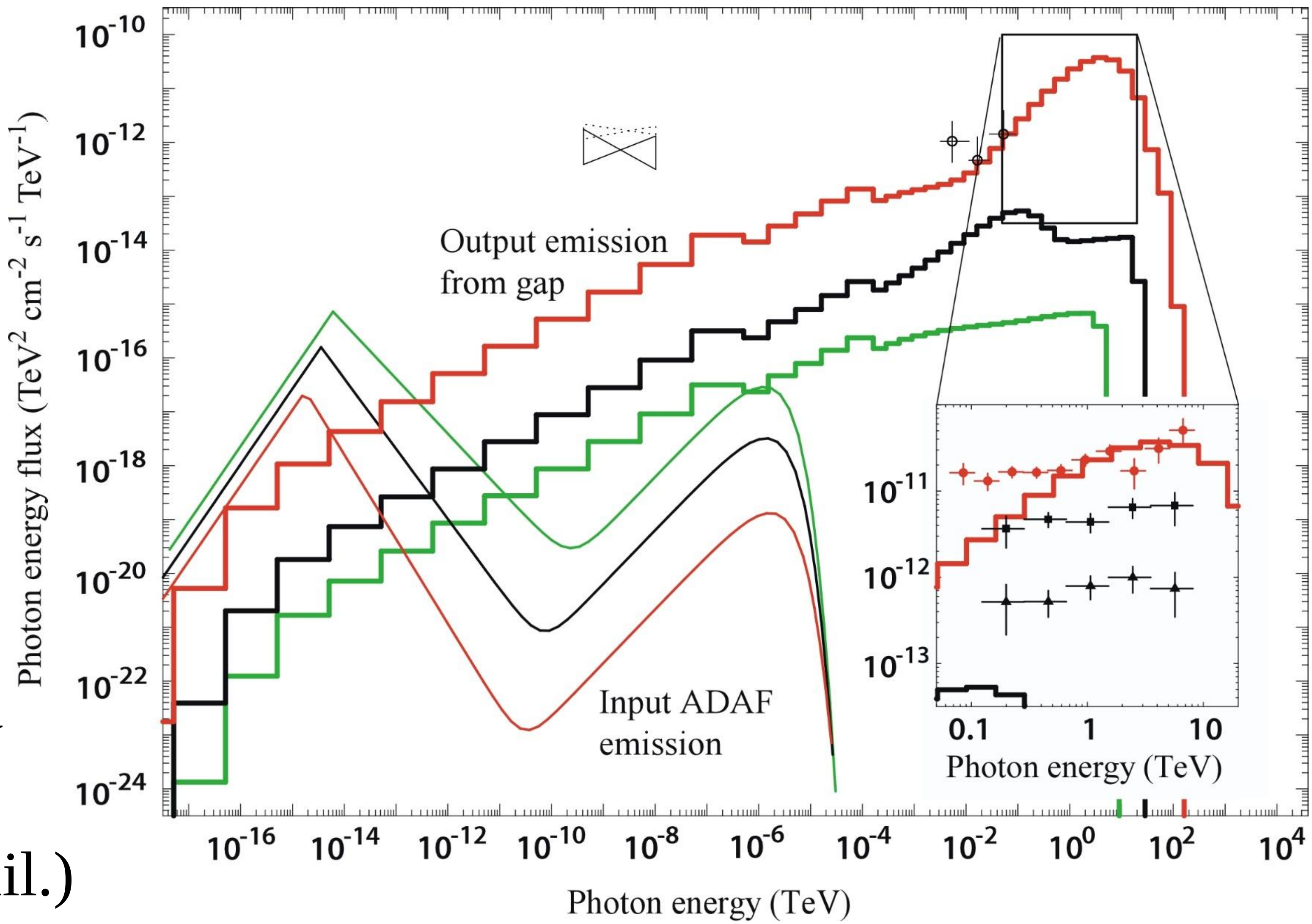

$B = 10^4$ G (fixed, not equil.)

§ 5 BH gap model

Small curvature radius, $R_c = 0.1r$.

KH & Pu 2015, submitted to ApJ

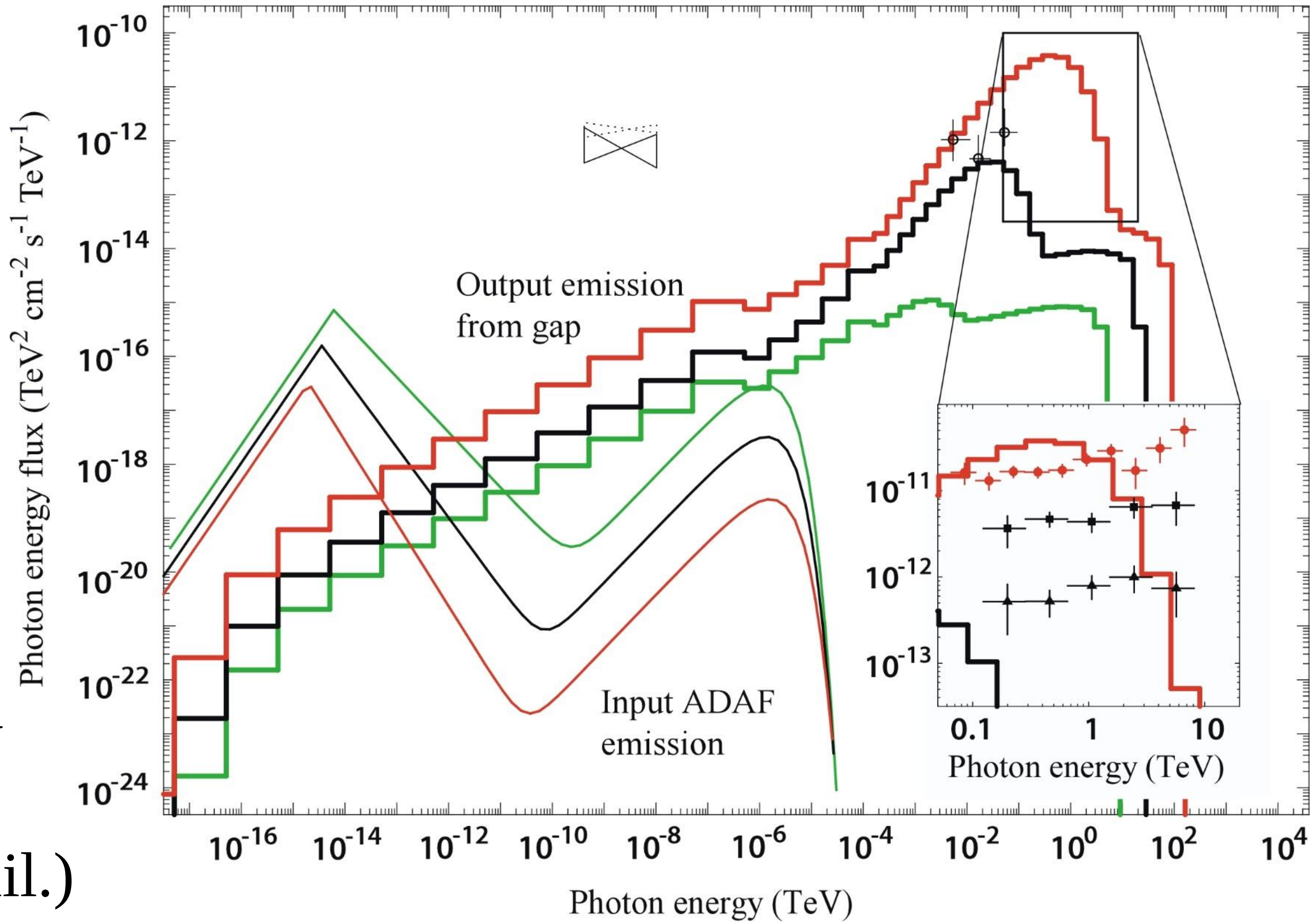

$B = 10^4$ G (fixed, not equil.)

§ 5 BH gap model

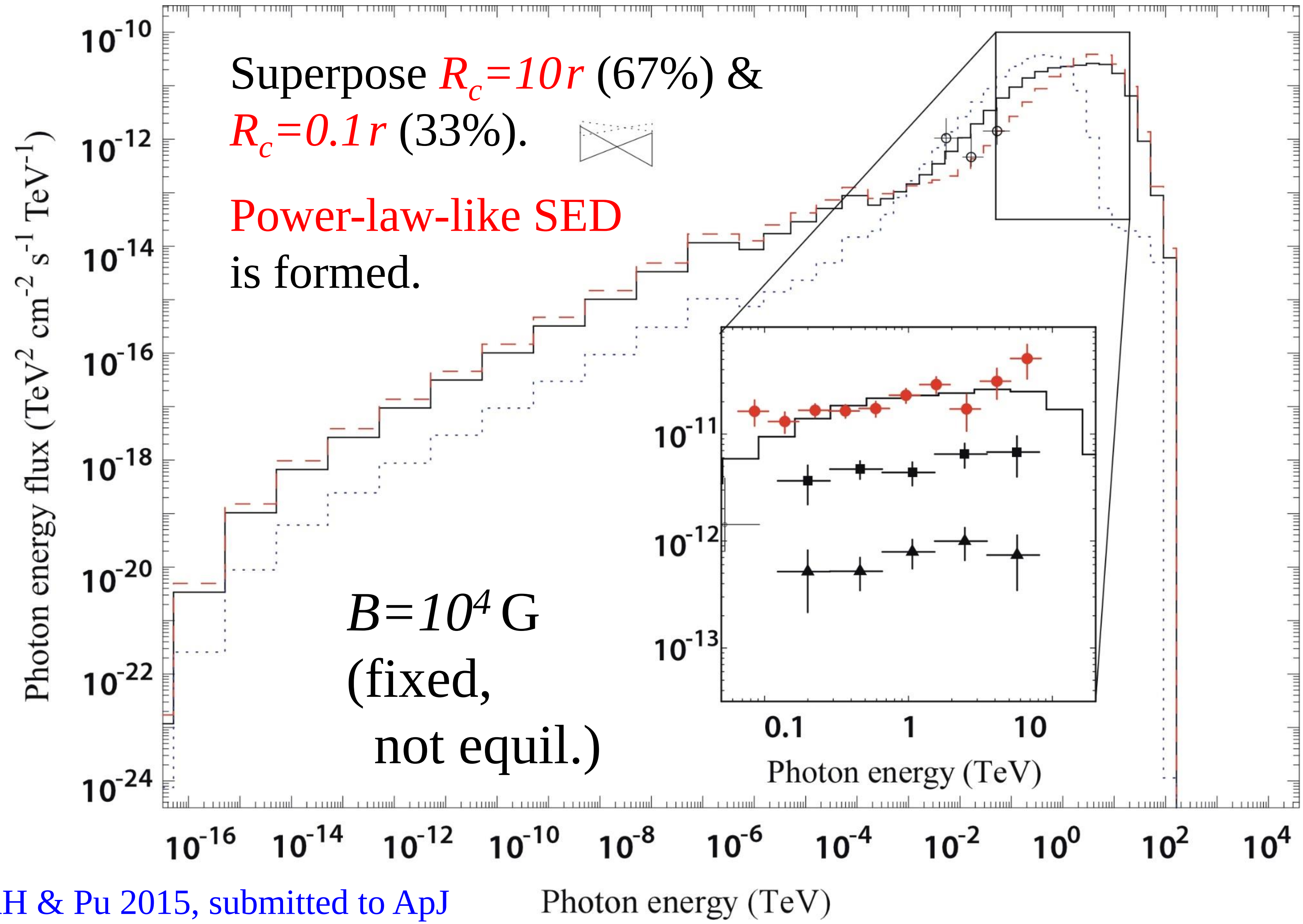

KH & Pu 2015, submitted to ApJ

Summary

HE/VHE emission from pulsar magnetospheres

- “Moderate ***B*** deformation (b~0.5) near LC is preferable to reproduce P1/P2 ratio and relatively large peak separation.
- Bridge emission reduces due to strong screening.
- $E_{||}$ screening in middle & lower altitudes naturally leads to outward-dominated outer-gap emission.

VHE emission from BH magnetospheres

- The VHE flare state of IC 310 can be reproduced w/ the BH gap model @ $\dot{M} = 4.9\times10^{-6}\,\dot{M}_{\rm Edd}$ for $a=0.998M$.
- The same method can be applied to other low-luminosity AGNs and to (stellar-mass) BH binaries.

Summary (cont'd)

Pulsar vs. BH gap models

- $E_{\parallel}$ sign is opposite between PSR and BH magnetospheres, because a null surface is formed by global $\boldsymbol{B}$ convex geometry in PSRs, but by the frame dragging in BHs.
- Soft photons are provided by NS surface thermal X-rays in PSR magnetospheres, but by accretion flow in BH ones.
- Accretion quenches gaps in PSRs, but switches on BHs, because $\beta \ll 1$ in PSRs, but $\beta \sim 1$ in BHs.
- HE/VHE emission is dependent on $\boldsymbol{B}$ geometry in PSRs, but independent in BHs, because null surface is formed by $\boldsymbol{B}$ geometry in PSRs but by frame dragging in BHs.